COMMUN. MATH. SCI.
Vol. 14, No. 3, pp. 831–855

THE RESPONSE OF REDUCED MODELS OF MULTISCALE DYNAMICS TO SMALL EXTERNAL PERTURBATIONS*

RAFAIL V. ABRAMOV† AND MARC KJERLAND‡

Abstract. In real-world geophysical applications (such as predicting climate change), the reduced models of real-world complex multiscale dynamics are used to predict the response of the actual multiscale climate to changes in various global atmospheric and oceanic parameters. However, while a reduced model may be adjusted to match a particular dynamical regime of a multiscale process, it is unclear why it should respond to external perturbations in the same way as the underlying multiscale process itself. In the current work, the authors study the statistical behavior of a reduced model of the linearly coupled multiscale Lorenz '96 system in the vicinity of a chosen dynamical regime by perturbing the reduced model via a set of forcing parameters and observing the response of the reduced model to these external perturbations. Comparisons are made to the response of the underlying multiscale dynamics to the same set of perturbations.

Key words. Multiscale dynamics, reduced models, response to external forcing.

AMS subject classifications. 37M, 37N.

1. Introduction

A reduced model for slow variables of multiscale dynamics is a lower-dimensional dynamical system, which "resolves" (that is, qualitatively approximates in some appropriate sense) major large scale slow variables of the underlying higher-dimensional multiscale dynamics while at the same time being relatively simple and computationally inexpensive to work with. This is important in real-world applications of contemporary science, such as geophysical science and climate change prediction [14,15,19,22,25,29,37], where the actual underlying physical process is impossible to model directly and its reduced approximation has to be designed for such a purpose. Reduced dynamics were used to model global circulation patterns [13, 18, 36, 48, 51] and large-scale features of tropical convection [24, 31]. Typically, reduced models of multiscale dynamics consist of simplified lower-dimensional dynamics of the original multiscale dynamics for the resolved variables, with additional terms and parameters which serve as replacements to the missing coupling terms with the unresolved variables of the underlying physical process. These extra parameters in the reduced model are usually computed to match a particular dynamical regime of the underlying multiscale dynamics [4, 6, 7, 12, 16, 17, 23, 32–35, 49]. In particular, if the underlying multiscale process changes its dynamical regime (for example, in response to changes in its own forcing parameters), then the parameters of the corresponding reduced model have to be appropriately readjusted to match its dynamical regime to the new regime of the multiscale dynamics.

In some real-world applications, such as climate change prediction, the reduced models of complex multiscale climate dynamics are used to predict the response of the actual multiscale climate to changes in various global atmospheric and oceanic parameters. However, while a reduced model may be manually adjusted to match a particular

*Received: May 3, 2013; accepted (in revised form): October 24, 2015. Communicated by Eric Vander-Eijnden.

†Department of Mathematics, Statistics and Computer Science, University of Illinois at Chicago, 851 S. Morgan st., Chicago, IL 60607 (abramov@math.uic.edu). http://www.math.uic.edu/~ abramov

‡Disaster Prevention Research Institute, Kyoto University, Gokasho, Uji 611-0011, Kyoto, Japan (marc.kjerland@gmail.com). http://www.marckjerland.com

dynamical regime of a multiscale process, it is unclear whether it should respond to identical external perturbations *a priori* in the same way as the multiscale process without any extra readjustments. How do reduced models of multiscale dynamics, adjusted to a particular dynamical regime, respond to external perturbations which force them out of this regime? Is their response similar to the response of the underlying multiscale dynamics to the same external perturbation? It is quite clear that the reduced dynamics evolve on a set with lower dimension than that of the full multiscale dynamics. How do the properties of this limiting set respond to changing the external forcing parameter in comparison to the full multiscale attractor?

Here, we develop a set of criteria for similarity of the response to small external perturbations between slow variables of multiscale dynamics and those of a reduced model for slow variables only, determined through statistical properties of the unperturbed dynamics. We carry out a computational study of these criteria in the linearly coupled rescaled Lorenz '96 model from [4, 7] as well as the difference in responses of the full multiscale and deterministic reduced dynamics of this system to identical external perturbations. Two different types of forcing perturbations are used: a Heaviside step forcing and a simple time-dependent ramp forcing. The manuscript is structured as follows. In Section 2, we formulate the standard averaging formalism to obtain the averaged slow dynamics from a general two-scale dynamical system. Section 3 describes statistically tractable criteria to ensure similarity of responses between a two-scale system and its averaged slow dynamics. In Section 4, we describe the first-order reduced model approximation to a two-scale dynamics with linear coupling between the slow and fast variables, previously developed in [4, 6, 7]. In Section 5, we introduce the two-scale Lorenz '96 toy model, which will be our testbed for this method. In Section 6, we present comparisons of the large features of the multiscale and reduced systems, including statistical comparisons as well as the ability of the reduced model to capture perturbation response of the multiscale system. Section 7 summarizes the results and suggests future work.

2. Averaged slow dynamics for a general two-scale system

A general two-scale dynamical system with slow variables $\boldsymbol{x}$ and fast variables $\boldsymbol{y}$ is usually represented as

$$\begin{cases} \dfrac{\mathrm{d}\boldsymbol{x}}{\mathrm{d}t} = \boldsymbol{F}(\boldsymbol{x},\boldsymbol{y}), \\ \dfrac{\mathrm{d}\boldsymbol{y}}{\mathrm{d}t} = \boldsymbol{G}(\boldsymbol{x},\boldsymbol{y}), \end{cases} \tag{2.1}$$

where $\boldsymbol{x}(t) \in \mathbb{R}^{N_x}$ are the slow variables of the system, $\boldsymbol{y}(t) \in \mathbb{R}^{N_y}$ are the fast variables, and $\boldsymbol{F}$ and $\boldsymbol{G}$ are nonlinear differentiable functions. The integer parameters $N_x \ll N_y$ are the dimensions of the slow and fast variable subspaces, respectively. Usually, a time-scale separation parameter is used to denote the difference in time scales between the slow and fast variables. However, we omit it here, as the framework for reduced models from [4, 6, 7] which we use here does not require such a parameter to be explicitly present.

Under the assumption of "infinitely fast" $\boldsymbol{y}$-variables, one can use the averaging formalism [38, 39, 46, 47] to write the averaged system for slow variables alone:

$$\frac{\mathrm{d}\boldsymbol{x}}{\mathrm{d}t} = \bar{\boldsymbol{F}}(\boldsymbol{x}), \qquad \bar{\boldsymbol{F}}(\boldsymbol{x}) = \int \boldsymbol{F}(\boldsymbol{x},\boldsymbol{y})\mathrm{d}\mu_{\boldsymbol{x}}(\boldsymbol{y}), \tag{2.2}$$

where $\mu_{\boldsymbol{x}}$ is the invariant distribution measure of the fast limiting system

$$\frac{\mathrm{d}\boldsymbol{z}}{\mathrm{d}\tau} = \boldsymbol{G}(\boldsymbol{x},\boldsymbol{z}), \tag{2.3}$$

with $\boldsymbol{x}$ above in (2.3) being a constant parameter. We express the slow solutions of the two-scale system in (2.1) and the averaged system in (2.2) in terms of differentiable flows:

$$\boldsymbol{x}(t) = \phi^t(\boldsymbol{x}_0,\boldsymbol{y}_0) \quad \text{for the two-scale system,} \tag{2.4a}$$

$$\boldsymbol{x}_A(t) = \phi_A^t(\boldsymbol{x}_0) \quad \text{for the averaged system.} \tag{2.4b}$$

It can be shown (see [38,39,46,47] and references therein) that if the time scale separation between $\boldsymbol{x}$ and $\boldsymbol{y}$ is large enough, then, for the identical initial conditions $\boldsymbol{x}_0$ and generic choice of $\boldsymbol{y}_0$, the solution $\boldsymbol{x}_A(t)$ of the averaged system in (2.2) remains near the solution $\boldsymbol{x}(t)$ of the original two-scale system in (2.1) for finitely long time.

3. Criteria of similarity of responses to small external perturbations for general two-scale system and its averaged slow dynamics

Let μ and μ_A denote the invariant distribution measures for the two-scale system in (2.1) and the averaged system in (2.2), respectively. Also, let $h(\boldsymbol{x})$ be a differentiable test function. Then, the statistically average values of h for both two-scale and averaged systems are given via

$$\langle h\rangle = \int h(\boldsymbol{x})\mathrm{d}\mu(\boldsymbol{x},\boldsymbol{y}), \tag{3.1a}$$

$$\langle h\rangle_A = \int h(\boldsymbol{x})\mathrm{d}\mu_A(\boldsymbol{x}). \tag{3.1b}$$

Now, consider the two-scale system in (2.1) and the averaged system in (2.2), perturbed at the slow variables by a small time-dependent forcing $\delta\boldsymbol{f}(t)$:

$$\begin{cases} \dfrac{\mathrm{d}\boldsymbol{x}}{\mathrm{d}t} = \boldsymbol{F}(\boldsymbol{x},\boldsymbol{y}) + \delta\boldsymbol{f}(t), \\ \dfrac{\mathrm{d}\boldsymbol{y}}{\mathrm{d}t} = \boldsymbol{G}(\boldsymbol{x},\boldsymbol{y}), \end{cases} \tag{3.2a}$$

$$\frac{\mathrm{d}\boldsymbol{x}}{\mathrm{d}t} = \bar{\boldsymbol{F}}(\boldsymbol{x}) + \delta\boldsymbol{f}(t). \tag{3.2b}$$

We similarly express the slow solutions of these perturbed systems in terms of differentiable flows:

$$\boldsymbol{x}^p(t) = \hat{\phi}^{t-s}(\boldsymbol{x}_0,\boldsymbol{y}_0,s), \tag{3.3a}$$

$$\boldsymbol{x}_A^p(t) = \hat{\phi}_A^{t-s}(\boldsymbol{x}_0,s). \tag{3.3b}$$

Then, the average responses $\delta\langle h\rangle(t)$ and $\delta\langle h\rangle_A(t)$ for the two-scale system in (2.1) and the averaged system in (2.2), respectively, are defined as

$$\delta\langle h\rangle(t) = \int h(\hat{\phi}^t(\boldsymbol{x},\boldsymbol{y},0))\mathrm{d}\mu(\boldsymbol{x},\boldsymbol{y}) - \langle h\rangle, \tag{3.4a}$$

$$\delta\langle h\rangle(t) = \int h(\hat{\phi}_A^t(\boldsymbol{x},0))\mathrm{d}\mu_A(\boldsymbol{x}) - \langle h\rangle_A, \tag{3.4b}$$

where, without loss of generality, we take $s=0$. The functional dependence of the responses $\delta\langle h\rangle(t)$ and $\delta\langle h\rangle_A(t)$ on $\delta\boldsymbol{f}$ may be complicated, but, for sufficiently small $\delta\boldsymbol{f}$, we expect the relationships to be linear. Then, the responses can be approximated by the following linear response relations:

$$\delta\langle h\rangle(t) \approx \int_0^t \boldsymbol{R}(t-s)\delta\boldsymbol{f}(s)\mathrm{d}s, \qquad \boldsymbol{R}(t) = \int \frac{\partial h(\phi^t(\boldsymbol{x},\boldsymbol{y}))}{\partial \boldsymbol{x}}\mathrm{d}\mu(\boldsymbol{x},\boldsymbol{y}), \tag{3.5a}$$

$$\delta\langle h\rangle_A(t) \approx \int_0^t \boldsymbol{R}_A(t-s)\delta\boldsymbol{f}(s)\mathrm{d}s, \qquad \boldsymbol{R}_A(t) = \int \frac{\partial h(\phi_A^t(\boldsymbol{x}))}{\partial \boldsymbol{x}}\mathrm{d}\mu_A(\boldsymbol{x}). \tag{3.5b}$$

For details, see Appendix A or [1–3, 8–11, 44]. Above, it is clear that any differences between $\delta\langle h\rangle(t)$ and $\delta\langle h\rangle_A(t)$ are due to differences between $\boldsymbol{R}(t)$ and $\boldsymbol{R}_A(t)$, since $\delta\boldsymbol{f}$ is identical in both cases. The differences between $\boldsymbol{R}(t)$ and $\boldsymbol{R}_A(t)$ are, in turn, caused by the differences between the flows ϕ^t and ϕ_A^t and the differences between the invariant distribution measures μ and μ_A, which are difficult to quantify in practice. In what follows, we express the differences between $\boldsymbol{R}(t)$ and $\boldsymbol{R}_A(t)$ via statistically tractable quantities. First, we assume that the invariant measures μ and μ_A are absolutely continuous with respect to the Lebesgue measure, with distribution densities $\rho(\boldsymbol{x},\boldsymbol{y})$ and $\rho_A(\boldsymbol{x})$, respectively:

$$\boldsymbol{R}(t) = \int \frac{\partial h(\phi^t(\boldsymbol{x},\boldsymbol{y}))}{\partial \boldsymbol{x}}\rho(\boldsymbol{x},\boldsymbol{y})\mathrm{d}\boldsymbol{x}\mathrm{d}\boldsymbol{y}, \tag{3.6a}$$

$$\boldsymbol{R}_A(t) = \int \frac{\partial h(\phi_A^t(\boldsymbol{x}))}{\partial \boldsymbol{x}}\rho_A(\boldsymbol{x})\mathrm{d}\boldsymbol{x}. \tag{3.6b}$$

While it is known that purely deterministic processes may not have Lebesgue-continuity of their invariant measures [42, 43, 50], even small amounts of random noise, which is always present in real-world complex geophysical dynamics, usually ensure the existence of the distribution density. Integration by parts yields

$$\boldsymbol{R}(t) = -\int h(\phi^t(\boldsymbol{x},\boldsymbol{y}))\frac{\partial \rho(\boldsymbol{x},\boldsymbol{y})}{\partial \boldsymbol{x}}\mathrm{d}\boldsymbol{x}\mathrm{d}\boldsymbol{y}, \tag{3.7a}$$

$$\boldsymbol{R}_A(t) = -\int h(\phi_A^t(\boldsymbol{x}))\frac{\partial \rho_A(\boldsymbol{x})}{\partial \boldsymbol{x}}\mathrm{d}\boldsymbol{x}. \tag{3.7b}$$

At this point, let us express $\rho(\boldsymbol{x},\boldsymbol{y})$ as the product of its marginal distribution $\bar{\rho}(\boldsymbol{x})$, defined as

$$\bar{\rho}(\boldsymbol{x}) = \int \rho(\boldsymbol{x},\boldsymbol{y})\mathrm{d}\boldsymbol{y}, \tag{3.8}$$

and conditional distribution $\rho(\boldsymbol{y}|\boldsymbol{x})$, given by

$$\rho(\boldsymbol{y}|\boldsymbol{x}) = \frac{\rho(\boldsymbol{x},\boldsymbol{y})}{\bar{\rho}(\boldsymbol{x})}. \tag{3.9}$$

It is easy to check that the conditional distribution $\rho(\boldsymbol{y}|\boldsymbol{x})$ satisfies the identity

$$\int \rho(\boldsymbol{y}|\boldsymbol{x})\mathrm{d}\boldsymbol{y} = 1 \quad \text{for all } \boldsymbol{x}. \tag{3.10}$$

Now, the formula for the linear response operator $\boldsymbol{R}(t)$ above can be written as

$$\boldsymbol{R}(t) = -\int h(\phi^t(\boldsymbol{x},\boldsymbol{y}))\rho(\boldsymbol{y}|\boldsymbol{x})\frac{\partial\bar{\rho}(\boldsymbol{x})}{\partial\boldsymbol{x}}\mathrm{d}\boldsymbol{y}\mathrm{d}\boldsymbol{x} - \int h(\phi^t(\boldsymbol{x},\boldsymbol{y}))\frac{\partial\rho(\boldsymbol{y}|\boldsymbol{x})}{\partial\boldsymbol{x}}\bar{\rho}(\boldsymbol{x})\mathrm{d}\boldsymbol{y}\mathrm{d}\boldsymbol{x}. \quad (3.11)$$

We now denote

$$\varepsilon^t(\boldsymbol{x},\boldsymbol{y}) = \phi^t(\boldsymbol{x},\boldsymbol{y}) - \phi^t_A(\boldsymbol{x}), \quad (3.12)$$

where $\varepsilon^t(\boldsymbol{x},\boldsymbol{y})$ is small compared to either $\phi^t(\boldsymbol{x},\boldsymbol{y})$ or $\phi^t_A(\boldsymbol{x})$ for relevant values of t, $\boldsymbol{x}$, and $\boldsymbol{y}$. Then, for the second integral in the right-hand side of (3.11) we write

$$\begin{aligned}
&-\int h(\phi^t(\boldsymbol{x},\boldsymbol{y}))\frac{\partial\rho(\boldsymbol{y}|\boldsymbol{x})}{\partial\boldsymbol{x}}\bar{\rho}(\boldsymbol{x})\mathrm{d}\boldsymbol{y} - \mathrm{d}\boldsymbol{x} \\
&= \int\left(\int\frac{\partial\rho(\boldsymbol{y}|\boldsymbol{x})}{\partial\boldsymbol{x}}\mathrm{d}\boldsymbol{y}\right) - h(\phi^t_A(\boldsymbol{x}))\bar{\rho}(\boldsymbol{x})\mathrm{d}\boldsymbol{x} - \int\nabla h(\phi^t_A(\boldsymbol{x})) - \varepsilon^t(\boldsymbol{x},\boldsymbol{y})\frac{\partial\rho(\boldsymbol{y}|\boldsymbol{x})}{\partial\boldsymbol{x}}\bar{\rho}(\boldsymbol{x}) \\
&\quad - \mathrm{d}\boldsymbol{y}\mathrm{d}\boldsymbol{x} = O(\|\varepsilon\|), \qquad (3.13)
\end{aligned}$$

where the first integral in the right-hand side is zero due to the condition in (3.10). Neglecting the $O(\|\varepsilon\|)$ terms in (3.7), we write

$$\boldsymbol{R}(t) = -\int h(\phi^t(\boldsymbol{x},\boldsymbol{y}))\rho(\boldsymbol{y}|\boldsymbol{x})\frac{\partial\bar{\rho}(\boldsymbol{x})}{\partial\boldsymbol{x}}\mathrm{d}\boldsymbol{y}\mathrm{d}\boldsymbol{x}, \quad (3.14a)$$

$$\boldsymbol{R}_A(t) = -\int h(\phi^t_A(\boldsymbol{x}))\frac{\partial\rho_A(\boldsymbol{x})}{\partial\boldsymbol{x}}\mathrm{d}\boldsymbol{x}. \quad (3.14b)$$

At this point, we express $\bar{\rho}(\boldsymbol{x})$ and $\rho_A(\boldsymbol{x})$ as exponentials:

$$\bar{\rho}(\boldsymbol{x}) = e^{-\bar{b}(\boldsymbol{x})}, \qquad \rho_A(\boldsymbol{x}) = e^{-b_A(\boldsymbol{x})}, \quad (3.15)$$

where $\bar{b}(\boldsymbol{x})$ and $b_A(\boldsymbol{x})$ are smooth functions, growing to infinity as $\boldsymbol{x}$ becomes infinite. The latter yields

$$\boldsymbol{R}(t) = \int h(\phi^t(\boldsymbol{x},\boldsymbol{y}))\frac{\partial\bar{b}(\boldsymbol{x})}{\partial\boldsymbol{x}}\rho(\boldsymbol{x},\boldsymbol{y})\mathrm{d}\boldsymbol{y}\mathrm{d}\boldsymbol{x}, \quad (3.16a)$$

$$\boldsymbol{R}_A(t) = \int h(\phi^t_A(\boldsymbol{x}))\frac{\partial b_A(\boldsymbol{x})}{\partial\boldsymbol{x}}\rho_A(\boldsymbol{x})\mathrm{d}\boldsymbol{x}. \quad (3.16b)$$

Replacing invariant measure averages with long-term time averages yields the following time-correlation functions:

$$\boldsymbol{R}(t) = \lim_{r\to\infty}\frac{1}{r}\int_0^r h(\boldsymbol{x}(s+t))\frac{\partial\bar{b}}{\partial\boldsymbol{x}}(\boldsymbol{x}(s))\mathrm{d}s, \quad (3.17a)$$

$$\boldsymbol{R}_A(t) = \lim_{r\to\infty}\frac{1}{r}\int_0^r h(\boldsymbol{x}_A(s+t))\frac{\partial b_A}{\partial\boldsymbol{x}}(\boldsymbol{x}_A(s))\mathrm{d}s. \quad (3.17b)$$

Taking into account the arbitrariness of h, we conclude that, in order for $\boldsymbol{R}_A(t)$ to approximate $\boldsymbol{R}(t)$ (despite the fact that, for long times s, $\boldsymbol{x}_A(s)$ diverges from $\boldsymbol{x}(s)$ even for identical initial conditions), we generally need three conditions to be approximately satisfied:

1. For identical initial conditions, $\boldsymbol{x}_A(t)$ should approximate $\boldsymbol{x}(t)$ (that is, $\varepsilon^t(\boldsymbol{x},\boldsymbol{y})$ in (3.12) should indeed be small) on the finite time scale of decay of the correlation functions in (3.17).

2. $b_A(\boldsymbol{x})$ should approximate $\bar{b}(\boldsymbol{x})$, which means that the invariant distribution $\rho_A(\boldsymbol{x})$ of the averaged system in (2.2) should be similar to the $\boldsymbol{x}$-marginal $\bar{\rho}(\boldsymbol{x})$ of the invariant distribution of the two-scale dynamical system in (2.1).

3. The timeautocorrelation functions of the averaged system in (2.2) should be similar to the time autocorrelation functions of the slow variables of the two-scale system in (2.1).

As a side note, observe that the nature of dependence of the conditional distribution $\rho(\boldsymbol{y}|\boldsymbol{x})$ on $\boldsymbol{x}$ does not play any role in the criteria for the similarity of responses. In particular, the exact factorization of $\rho(\boldsymbol{x},\boldsymbol{y})$ into its $\boldsymbol{x}$- and $\boldsymbol{y}$-marginals (which means that $\rho(\boldsymbol{y}|\boldsymbol{x})$ is independent of $\boldsymbol{x}$) is not required, unlike what was suggested in [30] for the Gaussian invariant states.

4. Practical implementation of the reduced model for a two-scale process with linear coupling

As formulated above in sections 2 and 3, the criteria of the response similarity are applicable for a broad range of dynamical systems with general forms of coupling and their averaged slow dynamics. However, the practical computation of the reduced model approximation to averaged slow dynamics depends on the form of coupling in the two-scale system [4, 6, 7]. In this work, we consider the linear coupling between the slow and fast variables in the two-scale system (2.1). The linear coupling is the most basic form of coupling in physical processes, and for that it is probably also the most common form of coupling. For the linear coupling, the reduced model is constructed according to the method developed previously in [4], which we briefly sketch below.

We consider the special setting of (2.1) with linear coupling between $\boldsymbol{x}$ and $\boldsymbol{y}$:

$$\begin{cases} \dfrac{\mathrm{d}\boldsymbol{x}}{\mathrm{d}t} = \boldsymbol{f}(\boldsymbol{x}) + \boldsymbol{L}_y\boldsymbol{y}, \\ \dfrac{\mathrm{d}\boldsymbol{y}}{\mathrm{d}t} = \boldsymbol{g}(\boldsymbol{y}) + \boldsymbol{L}_x\boldsymbol{x}, \end{cases} \tag{4.1}$$

where $\boldsymbol{f}$ and $\boldsymbol{g}$ are nonlinear differentiable functions and $\boldsymbol{L}_x$ and $\boldsymbol{L}_y$ are constant matrices of appropriate sizes. The corresponding averaged dynamics for slow variables from (2.2) simplifies to

$$\frac{\mathrm{d}\boldsymbol{x}}{\mathrm{d}t} = \boldsymbol{f}(\boldsymbol{x}) + \boldsymbol{L}_y\bar{\boldsymbol{z}}(\boldsymbol{x}), \tag{4.2}$$

where $\bar{\boldsymbol{z}}(\boldsymbol{x})$ is the statistical mean state of the fast limiting system

$$\frac{\mathrm{d}\boldsymbol{z}}{\mathrm{d}\tau} = \boldsymbol{g}(\boldsymbol{z}) + \boldsymbol{L}_x\boldsymbol{x}, \tag{4.3}$$

with $\boldsymbol{x}$ treated as constant parameter. In general, the exact dependence of $\bar{\boldsymbol{z}}(\boldsymbol{x})$ on $\boldsymbol{x}$ is unknown, except for a few special cases like the Ornstein–Uhlenbeck process [45]. Here, like in [4, 7], we approximate $\bar{\boldsymbol{z}}(\boldsymbol{x})$ via the linear expansion

$$\bar{\boldsymbol{z}}(\boldsymbol{x}) \approx \bar{\boldsymbol{z}}^* + \boldsymbol{\mathcal{C}}\boldsymbol{L}_x(\boldsymbol{x} - \boldsymbol{x}^*), \tag{4.4}$$

where $\boldsymbol{x}^*$ is the statistical average state of the full multiscale system in (4.1) or another appropriate reference state, and where $\bar{\boldsymbol{z}}^* = \bar{\boldsymbol{z}}(\boldsymbol{x}^*)$. The constant matrix $\boldsymbol{\mathcal{C}}$ is computed as the time integral of the correlation function

$$\boldsymbol{\mathcal{C}} = \left(\int_0^t \boldsymbol{C}(s) \mathrm{d}s \right) \boldsymbol{C}^{-1}(0), \qquad \boldsymbol{C}(s) = \lim_{r \to \infty} \frac{1}{r} \int_0^r \boldsymbol{z}(t+s) \boldsymbol{z}^T(t) \mathrm{d}t, \tag{4.5}$$

where $\boldsymbol{z}(t)$ is the solution of (4.3) for $\boldsymbol{x} = \boldsymbol{x}^*$. For the details of this calculation, see Appendix B. The above formula constitutes the quasi-Gaussian approximation to the linear response of $\bar{\boldsymbol{z}}$ to small constant forcing perturbations in (4.3), and is a good approximation when the dynamics in (4.3) are strongly chaotic and rapidly mixing [1–3,8–11,28,40]. With (4.5), the reduced system in (4.2) becomes the explicitly defined deterministic reduced model for slow variables alone:

$$\frac{\mathrm{d}\boldsymbol{x}}{\mathrm{d}t} = \boldsymbol{f}(\boldsymbol{x}) + \boldsymbol{L}_y \bar{\boldsymbol{z}}^* + \boldsymbol{L}_y \boldsymbol{\mathcal{C}} \boldsymbol{L}_x (\boldsymbol{x} - \boldsymbol{x}^*). \tag{4.6}$$

In what follows, the "zero-order" model refers to (4.6) with the last term set to zero (such that the coupling is parameterized only by the constant term $\boldsymbol{L}_y \bar{\boldsymbol{z}}^*$):

$$\frac{\mathrm{d}\boldsymbol{x}}{\mathrm{d}t} = \boldsymbol{f}(\boldsymbol{x}) + \boldsymbol{L}_y \bar{\boldsymbol{z}}^*. \tag{4.7}$$

For details, see [4, 7] and references therein.

5. Testbed – the Lorenz '96 system

In the current work, we test the statistical similarity criteria and response of the reduced model for slow variables on a rescaled Lorenz '96 system with linear coupling [4], which is obtained from the two-scale Lorenz '96 system [27] by appropriately rescaling the dynamical variables to approximately set their mean states and variances to zero and one, respectively. Below, we present a brief exposition of how the rescaled Lorenz '96 model is derived.

5.1. The two-scale Lorenz '96 system. In an exposition on predictability in atmospheric-type systems [27], Lorenz proposed the system

$$\dot{x}_i = x_{i-1}(x_{i+1} - x_{i-2}) - x_i + F, \qquad i = 1, \ldots, N, \tag{5.1}$$

with periodic boundary conditions. This system has generic features of geophysical flows, namely a nonlinear advection-like term, linearly unstable waves, damping, forcing, mixing, and chaos [28]. The simple formulation, with invariance under index translation and a uniform forcing term F, allows for straightforward analysis. In particular the long-time statistics of each variable are identical and depend only on F. Additionally, the chaos and mixing of the system are dictated by the forcing, with decaying solutions for F near zero, periodic solutions for F slightly larger, weakly chaotic quasi-periodic solutions around $F = 6$, and chaotic and strongly mixing systems around $F = 16$ and higher.

To study predictability and Lyapunov exponents for systems with subgrid phenomena operating on faster timescales, Lorenz proposed the two-time system given by

$$\begin{cases} \dot{x}_i = x_{i-1}(x_{i+1} - x_{i-2}) - x_i + F_x - \dfrac{\lambda_y}{J} \displaystyle\sum_{j=1}^{J} y_{i,j}, \\ \dot{y}_{i,j} = \dfrac{1}{\varepsilon} \left[y_{i,j+1}(y_{i,j-1} - y_{i,j+2}) - y_{i,j} + F_y + \lambda_x x_i \right], \end{cases} \tag{5.2}$$

referred to as the Lorenz '96 system, where $1 \le i \le N_x, 1 \le j \le J$, with periodic boundary conditions $x_{i+N_x} = x_i$, $y_{i+N_x,j} = y_{i,j}$, and $y_{i,j+J} = y_{i+1,j}$. Here, F_x and F_y are constant forcing terms, λ_x and λ_y constant coupling parameters, and ε is the explicit time scale separation parameter. In Lorenz's original formulation, $F_y \equiv 0$, but here we take $F_y \gg 0$ to force the fast system into a chaotic regime.

5.2. Rescaling the Lorenz '96 system. To further simplify the analysis of coupling trends for the two-time system, we will scale out the dependence of the mean state and mean energy on the forcing term F. Due to the translational invariance, the long-term mean $\overline{x}$ and standard deviation σ for the uncoupled system (5.1) are the same for all x_i. So, we rescale $\boldsymbol{x}$ and t as

$$x_i = \overline{x} + \sigma \hat{x}_i, \quad t = \frac{\tau}{\sigma}, \tag{5.3}$$

where the new variables $\hat{x}$ have zero mean and unit standard deviation, while their time autocorrelation functions have normalized scaling across different dynamical regimes (that is, different forcings F) for short correlation times. This rescaling was previously used in [28]. In the rescaled variables, the uncoupled Lorenz model becomes

$$\dot{\hat{x}}_i = \left(\hat{x}_{i-1} + \frac{\overline{x}}{\sigma}\right)(\hat{x}_{i+1} - \hat{x}_{i-2}) - \frac{\hat{x}_i}{\sigma} + \frac{F - \overline{x}}{\sigma^2}, \tag{5.4}$$

where $\overline{x}$ and σ are functions of F, determined numerically.

We similarly rescale the coupled two-scale Lorenz '96 model:

$$\begin{cases} \dfrac{\mathrm{d}x_i}{\mathrm{d}t} = \left(x_{i-1} + \dfrac{\overline{x}}{\sigma_x}\right)(x_{i+1} - x_{i-2}) - \dfrac{x_i}{\sigma_x} + \dfrac{F_x - \overline{x}}{{\sigma_x}^2} - \dfrac{\lambda_y}{J}\displaystyle\sum_{j=1}^{J} y_{i,j}, \\ \varepsilon \dfrac{\mathrm{d}y_{i,j}}{\mathrm{d}t} = \left(y_{i,j+1} + \dfrac{\overline{y}}{\sigma_y}\right)(y_{i,j-1} - y_{i,j+2}) - \dfrac{y_{i,j}}{\sigma_y} + \dfrac{F_y - \overline{y}}{{\sigma_y}^2} + \lambda_x x_i, \end{cases} \tag{5.5}$$

where $\{\overline{x},\ \sigma_x\}$ and $\{\overline{y},\ \sigma_y\}$ are the long-term means and standard deviations of the uncoupled systems with F_x or F_y as constant forcing, respectively. It is this rescaled coupled Lorenz '96 system that we focus on for the closure approximation.

Before any numerical tests, one can already anticipate that the zero-order reduced system will be inadequate for this model even with such simple coupling. Once the reference state $\boldsymbol{x}^*$ is determined and $\overline{\boldsymbol{z}}^*$ computed, the zero-order reduced system is given, according to (4.6), by

$$\dot{\hat{x}}_i = \left(\hat{x}_{i-1} + \frac{\overline{x}}{\sigma}\right)(\hat{x}_{i+1} - \hat{x}_{i-2}) - \frac{\hat{x}_i}{\sigma} + \frac{F - \overline{x}}{\sigma^2} - \lambda_y \overline{z}^*. \tag{5.6}$$

This is equivalent to perturbing F_x by $-\sigma_x^2 \lambda_y \overline{z}^*$, which we expect to be small since $\hat{x}$ and $\hat{y}$ have zero mean in the uncoupled setting. In particular, we expect this perturbation to have only a small effect on the dynamics. However, in the multiscale dynamics, it has been shown that a chaotic regime in the fast system can suppress chaos when coupled to the slow system [5], and this phenomenon is completely lost in the zero-order model.

6. Numerical experiments

In this part of the study, we compare the numerical results of the rescaled two-scale Lorenz '96 system with its corresponding reduced systems, with and without the linear correction term. In particular, we look at the ability of the reduced system to capture

some statistical quantities and how well it captures response to perturbations in the slow variables.

In all parameter regimes considered, we have a slow system consisting of twenty variables ($N_x = 20$) coupled with a fast system of eighty variables ($N_y = 80$). We use a fourth-order Runge–Kutta method with timestep $dt = \varepsilon/10$ in the multiscale system and $dt = 1/10$ in the reduced system. To compute the mean response ($h(\boldsymbol{x}) = \boldsymbol{x}$ in (3.4)) an ensemble of 10^4 points is generated by sampling from a single trajectory which has been given sufficient time to settle onto the attractor. Using the translational symmetry of the Lorenz '96 system, for each member of the ensemble, we rotate the indices to generate an ensemble twenty times larger.

On a modern laptop, the initial calculation to generate the reduced system for the Lorenz '96 system takes only a few minutes. Once computed, a numerical simulation of the reduced system is faster than the multiscale system by a factor of ε^{-1}. Computing the mean response for a single forcing for five time units with a sufficiently large ensemble size (10^5 trajectories) takes over an hour in the multiscale system with $\varepsilon = 10^{-2}$ but less than three minutes for the corresponding reduced system.

6.1. Comparison of statistical properties of the two-scale and reduced systems. In Section 3, we outlined the main requirements for correctly capturing the response of the two-scale system by its reduced model. Those were the approximation of joint distribution density functions (DDF) for slow variables and the time autocorrelation functions of the time series. It is, of course, not computationally feasible to directly compare the 20-dimensional DDFs and time autocorrelations for all possible test functions. However, it is possible to compare the one-dimensional marginal DDFs and simple time autocorrelations for individual slow variables, and thus have a rough estimate on how the statistical properties of the multiscale dynamics are reproduced by the reduced model.

In Figure 6.1, we compare the distribution density functions and autocorrelation functions of the slow variables. The DDFs are computed using bin-counting, and the autocorrelation function $\langle x_i(t)x_i(t+s)\rangle$, averaged over t, is normalized by the variance $\langle x_i^2\rangle$. Results from three parameter regimes are presented, and, in all three regimes, the fast system is chaotic and weakly mixing ($F_y = 12$) and the coupling strength is chosen to be large enough ($\lambda_x = \lambda_y = 0.4$) so that the multiscale dynamics are challenging to approximate. Of particular interest are timescale separations of $\varepsilon = 10^{-1}$ and $\varepsilon = 10^{-2}$.

First, we consider a chaotic and strongly mixing slow regime ($F_x = 16$). Figures are presented for the timescale separation $\varepsilon = 10^{-1}$ only, because, in this regime, the situation is very similar for $\varepsilon = 10^{-2}$. We also consider a weakly chaotic and quasi-periodic slow regime ($F_x = 8$). In this regime, the coupled dynamics are more dependent on the timescale separation, so we present results for both $\varepsilon = 10^{-1}$ and $\varepsilon = 10^{-2}$. Statistical quantities of other regimes, including those with less chaotic behavior, have been presented in [4].

To more systematically compare DDFs for many parameter regimes, we introduce two metrics on the space of distributions. First is the Jensen–Shannon metric, which is derived from the information-theoretic Kullback–Leibler divergence [26] and given by

$$m_{\mathrm{JS}}(P,Q) = \frac{1}{\sqrt{2}}\left(\int_{-\infty}^{\infty} \log\left(\frac{2p(x)}{p(x)+q(x)}\right) p(x)dx + \int_{-\infty}^{\infty} \log\left(\frac{2q(x)}{p(x)+q(x)}\right) q(x)dx\right)^{1/2}, \tag{6.1}$$

where p and q are densities on distributions P and Q. This metric represents to some extent the relative entropy of the distributions and provides a sense of the amount of

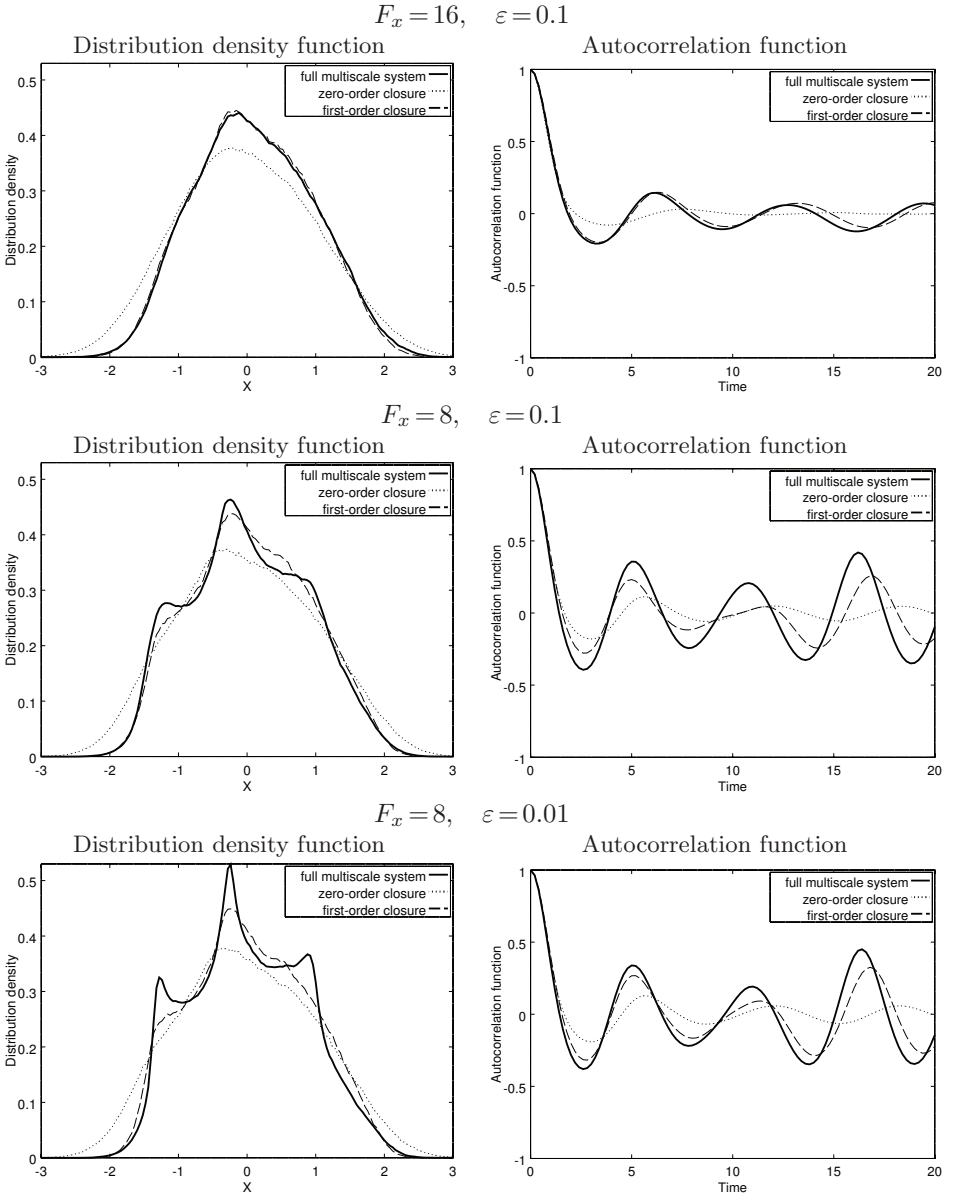

FIG. 6.1. *Distribution density and autocorrelation functions of slow variables.*

information lost by using one distribution in place of the other. The next metric we consider is the earth mover's distance [41], also known as the first Wasserstein metric. Motivated by transportation theory, this metric measures the minimum work needed to move one distribution function to another as though they were piles of dirt, the energy cost is the amount of 'dirt' times the Euclidean ground distance it moved. For distribution functions of one-dimensional random variables, the earth mover's distance is the L^1 norm of the difference of the cumulative distributions:

$$m_{\mathrm{EM}}(P,Q) = \int_{-\infty}^{\infty} \left| \int_{-\infty}^{x} p(s) - q(s) \mathrm{d}s \right| \mathrm{d}x. \tag{6.2}$$

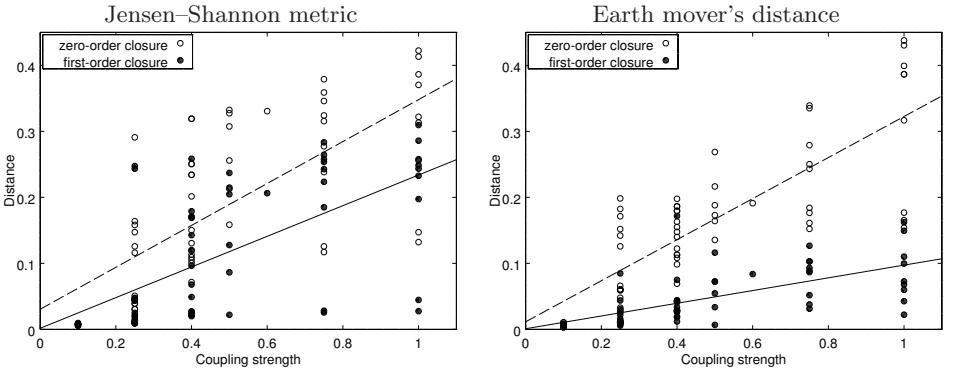

FIG. 6.2. *Distances between DDFs of reduced and multiscale systems, with linear best fit for the zero-order system (dashed line) and first-order system (solid line).*

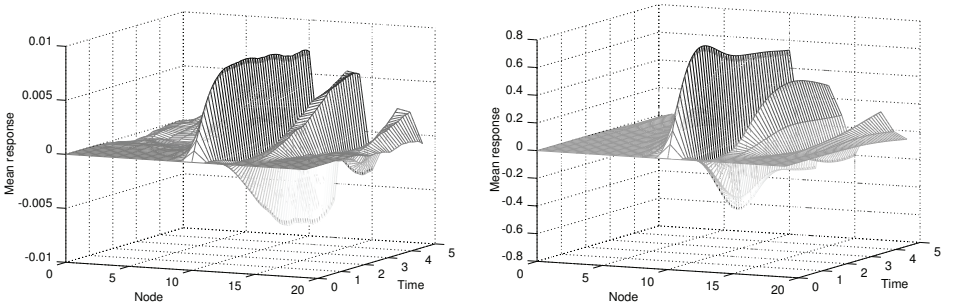

FIG. 6.3. *Response of* $\langle \boldsymbol{x} \rangle$ *(*$h(\boldsymbol{x}) = \boldsymbol{x}$ *in* (3.4)*) to Heaviside step forcing* $\delta f = 0.01$ *(left)* $\delta f = 1$ *(right) and at node* x_{11} *in a chaotic regime of the two-time rescaled Lorenz '96 system.* $N_x = 20$, $N_y = 80$, $F_x = 16$, $F_y = 12$, $\lambda_x = 0.4$, $\lambda_y = 0.4$, $\varepsilon = 0.1$

This is has the particularly intuitive property that the earth mover's distance between two delta distributions δ_α and δ_β is simply the distance between their centers $|\alpha - \beta|$.

Figure 6.2 shows distances between reduced systems DDFs and the corresponding multiscale slow variable DDFs. A variety of regimes is considered, with coupling parameters $\lambda_x, \lambda_y \in [0.1, 1]$, forcing parameters $F_x \in \{6, 7, 8, 10, 16\}$ and $F_y \in \{8, 12, 16\}$, and timescale separations $\varepsilon \in \{10^{-1}, 10^{-2}\}$. The data points are plotted with respect to coupling parameter λ_x. For each regime considered, the corresponding distances are shown for both zero-order and first-order reduced systems. As the coupling strength between fast and slow systems increases, it is apparently more difficult for the reduced systems to capture the correct slow dynamics of the multiscale system. It should be noted that this correlation is slightly weaker when plotted against λ_y, the coupling parameter for the fast system. However, the distribution densities of the first-order reduced system are consistently closer in both metrics than the zero-order system to the multiscale system.

6.2. Mean state response to forcing perturbations. In this section we examine the response of the mean state $\langle \boldsymbol{x} \rangle$ of the slow variables $\delta \langle \boldsymbol{x} \rangle(t)$ (that is, $h(\boldsymbol{x}) = \boldsymbol{x}$ in (3.1)) in the Lorenz '96 system to two simple types of external forcing:

1. Heaviside step forcing

$$\delta \boldsymbol{f}_{\mathrm{H}}(t) = \begin{cases} \boldsymbol{v} & \text{if } t > 0, \\ 0 & \text{if } t < 0, \end{cases} \tag{6.3}$$

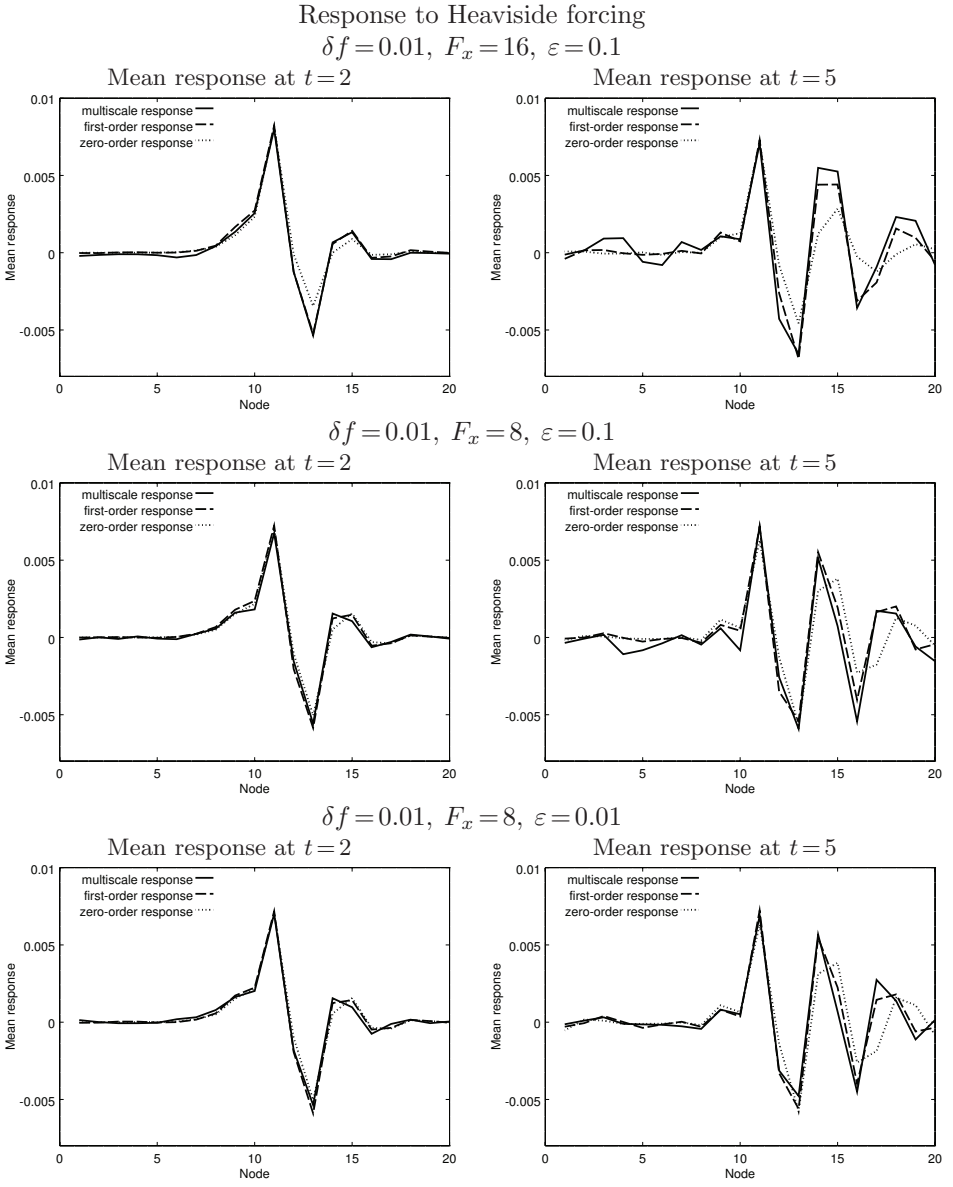

FIG. 6.4. *Snapshots of the mean response* $\delta\langle \boldsymbol{x}\rangle(t)$ *(*$h(\boldsymbol{x}) = \boldsymbol{x}$ *in* (3.4)*) to small Heaviside forcing* $\delta f = 0.01$ *at time* $t = 2$ *(left), and* $t = 5$ *(right).*

2. Ramp forcing

$$\delta \boldsymbol{f}_r(t) = \begin{cases} \boldsymbol{v} & \text{if } t > t_r, \\ \boldsymbol{v}t/t_r & \text{if } 0 < t < t_r, \\ 0 & \text{if } t < 0, \end{cases} \tag{6.4}$$

where $\boldsymbol{v}$ is a constant vector and t_r is a fixed time when the ramp forcing reaches its maximum. To compute the response of the mean state $\langle \boldsymbol{x}\rangle$, we generate an initial ensemble sampled from a trajectory that has been given sufficient time to settle onto

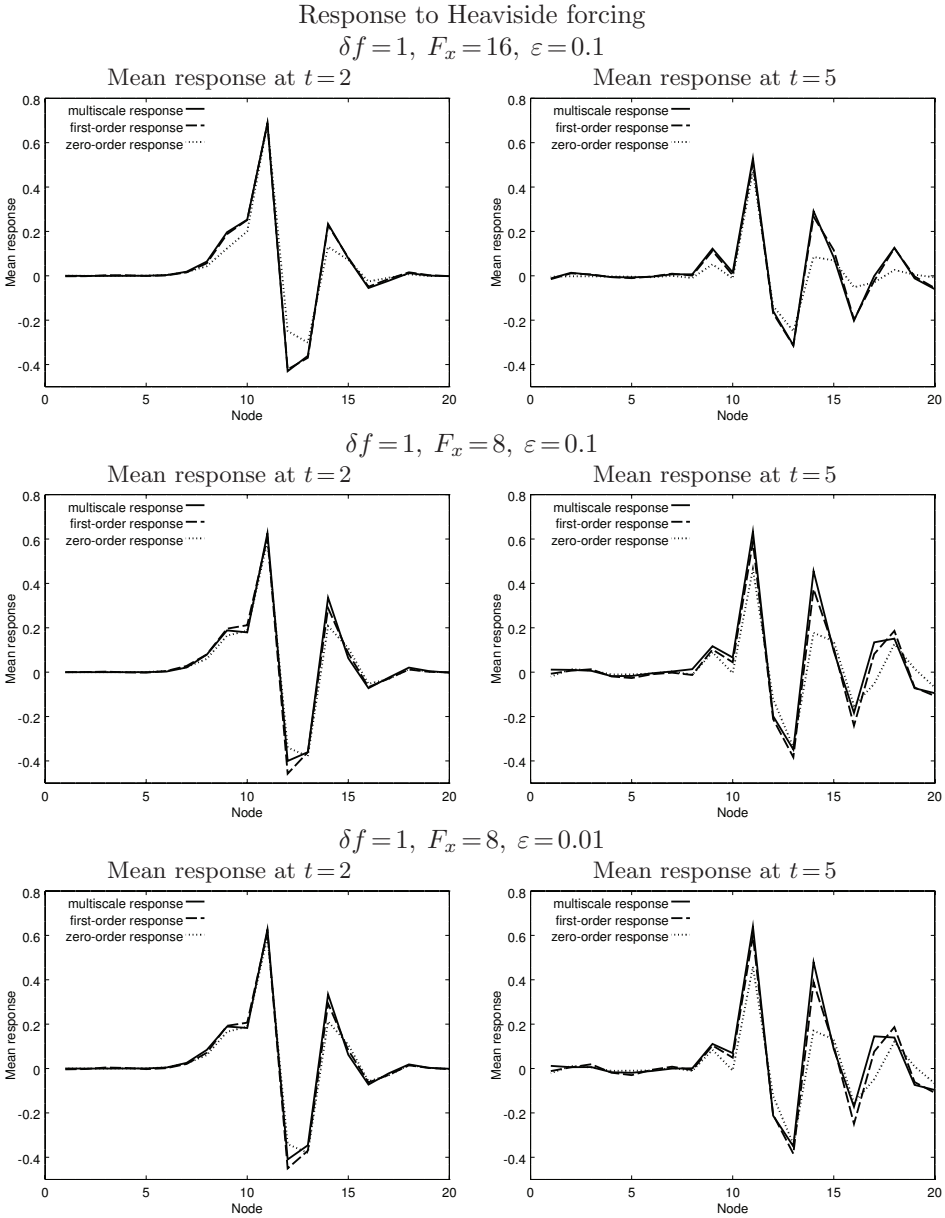

FIG. 6.5. *Snapshots of the mean response* $\delta\langle \boldsymbol{x}\rangle(t)$ *(*$h(\boldsymbol{x}) = \boldsymbol{x}$ *in* (3.4)*) to large Heaviside forcing* $\delta f = 1$ *at time* $t = 2$ *(left) and* $t = 5$ *(right).*

the attractor. For each ensemble member, we compute a short trajectory under the unperturbed dynamics as well as the under the perturbed dynamics, and then we take the difference between these two trajectories and average over the entire ensemble. Here, we consider forcing of the form $\boldsymbol{v} = \delta f \cdot \hat{e}_j$, where δf is a scalar constant and $\hat{e}_j$ a standard basis vector in $\mathbb{R}^{N_x}$. For the translation-invariant Lorenz '96 system, we only consider forcing at a single node.

The plots in Figure 6.3 show the response of the slow variables mean state $\delta\langle \boldsymbol{x}\rangle$

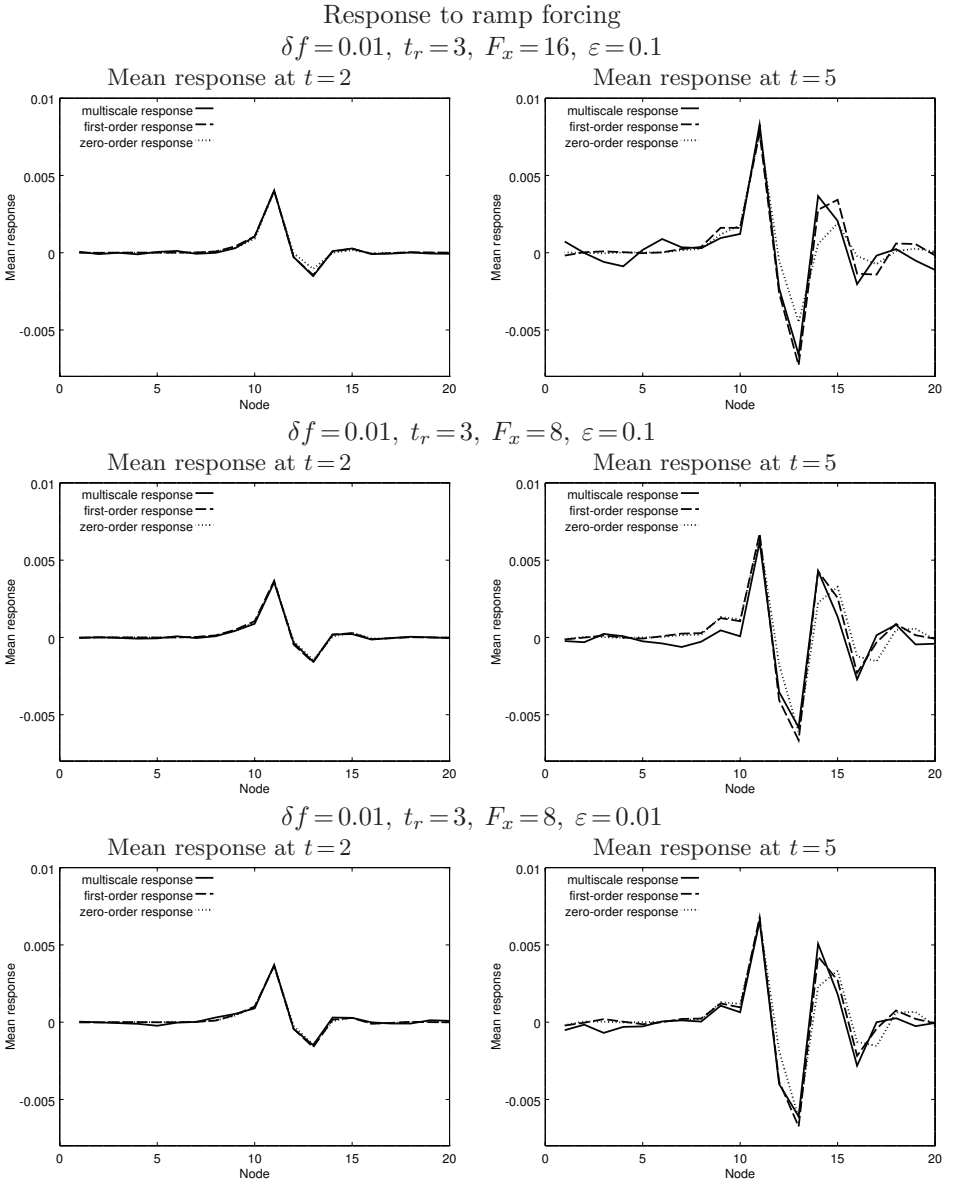

FIG. 6.6. *Snapshots of the mean response* $\delta\langle \boldsymbol{x}\rangle(t)$ *(*$h(\boldsymbol{x}) = \boldsymbol{x}$ *in* (3.4)*) to small ramp forcing* $\delta f = 0.01,\ t_r = 3$ *at time* $t = 2$ *(left) and* $t = 5$ *(right).*

to small Heaviside forcing of magnitudes $\delta f = 0.01$ and $\delta f = 1$ at node $x_{11}$for five time units, averaged over an ensemble of size 200,000. For comparison, the average magnitude of the right-hand side for this parameter regime is $\langle |\frac{\mathrm{d}\boldsymbol{x}}{\mathrm{d}t}| \rangle = \langle |\boldsymbol{F}| \rangle = 0.38$. In these plots we can see the primary response in the forced node as well as the propagation of the response to the adjacent nodes in the direction of advection. Here, the large features of the Heaviside forcing mean response are mostly developed after five time units and provide a good indication of the infinite time response.

We now compare the mean response of the full and reduced systems. Figures 6.4 and

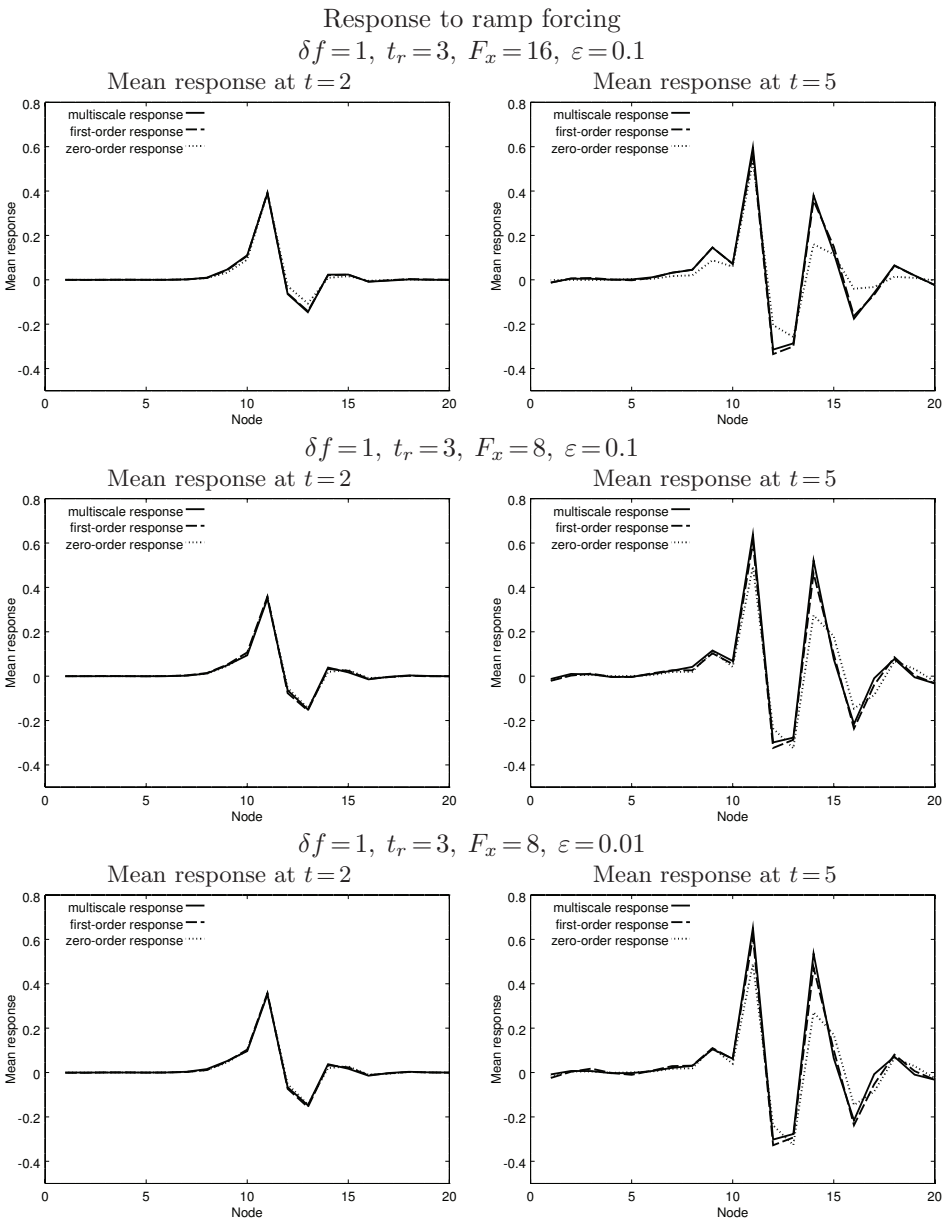

FIG. 6.7. *Snapshots of the mean response* $\delta\langle \boldsymbol{x}\rangle(t)$ *(*$h(\boldsymbol{x}) = \boldsymbol{x}$ *in* (3.4)*) to large ramp forcing* $\delta f = 1,\ t_r = 3$ *at time* $t = 2$ *(left) and* $t = 5$ *(right).*

6.5 show snapshots of the mean responses for the two-scale and reduced models at times $t = 2$ and $t = 5$ with the Heaviside forcing of $\delta f = 0.01$ and $\delta f = 1$, respectively. Response to ramp forcing is shown in figures 6.6 and 6.7, where the forcing increases linearly from zero for $t_r = 3$ time units to a maximum of $\delta f = 0.01$ and $\delta f = 1$, respectively.

In all these plots, the reduced models capture quite closely the response of the node which is directly perturbed, but they differ in their ability to capture the responses of the remaining nodes. In the case of larger forcing $\delta f = 1$, the first-order model responds

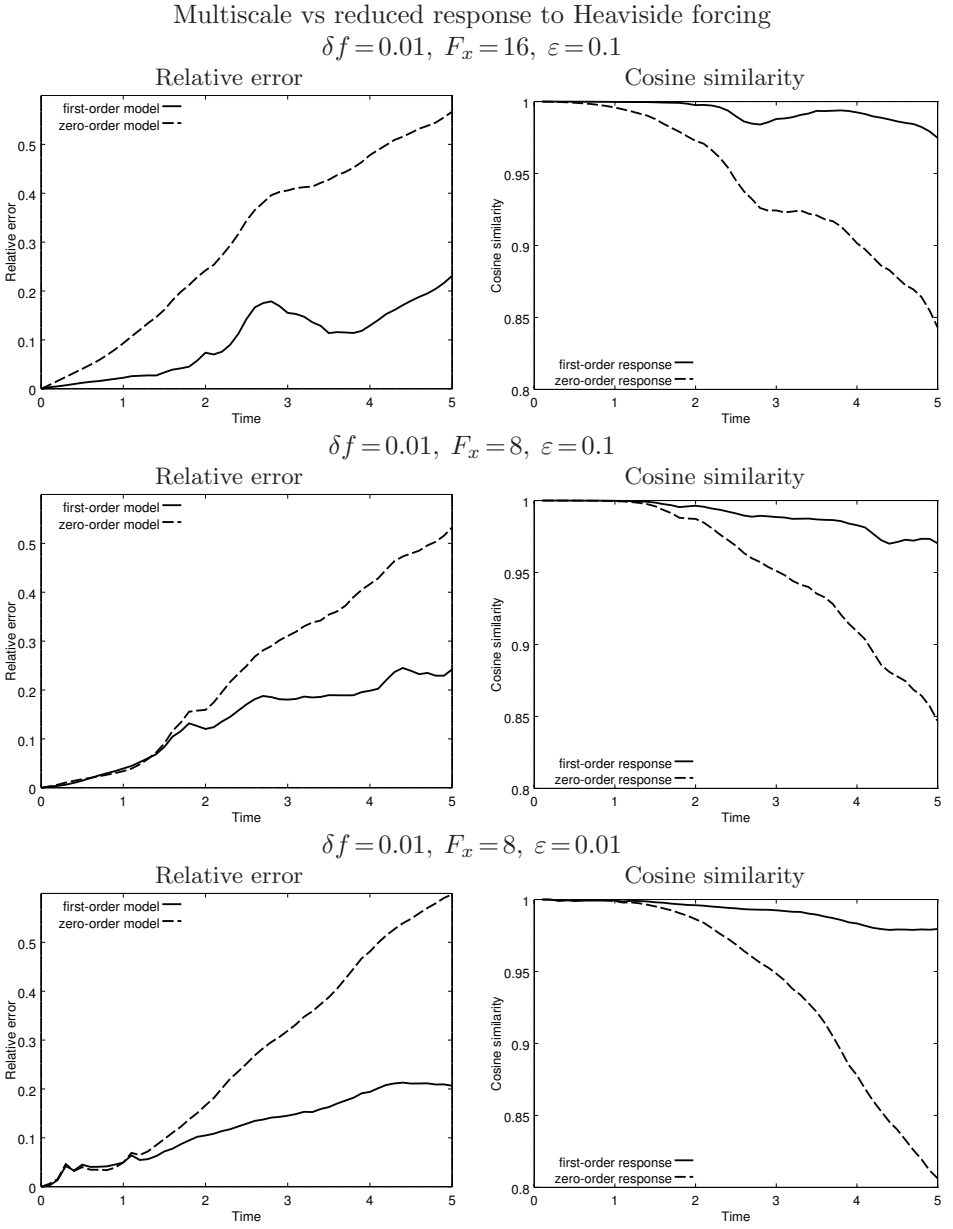

FIG. 6.8. *Comparison of multiscale and reduced system mean responses* $\delta\langle \boldsymbol{x} \rangle(t)$ *to Heaviside forcing. Relative error* (6.5) *on the left, cosine similarity* (6.6) *on the right.*

closely to the multiscale system, while the zero-order model tends to underrepresent the response. When the forcing is small, the small oscillations that propagate in the multiscale system are relatively large compared to the linear response, and this is a purely multiscale phenomenon that the reduced models are unable to capture. Note that this difference is less prominent as the timescale separation increases ($\varepsilon \to 0$), allowing sufficient time for the oscillations to dissipate in the strongly mixing fast system.

For a quantitative comparison of these responses, we plot the relative error versus

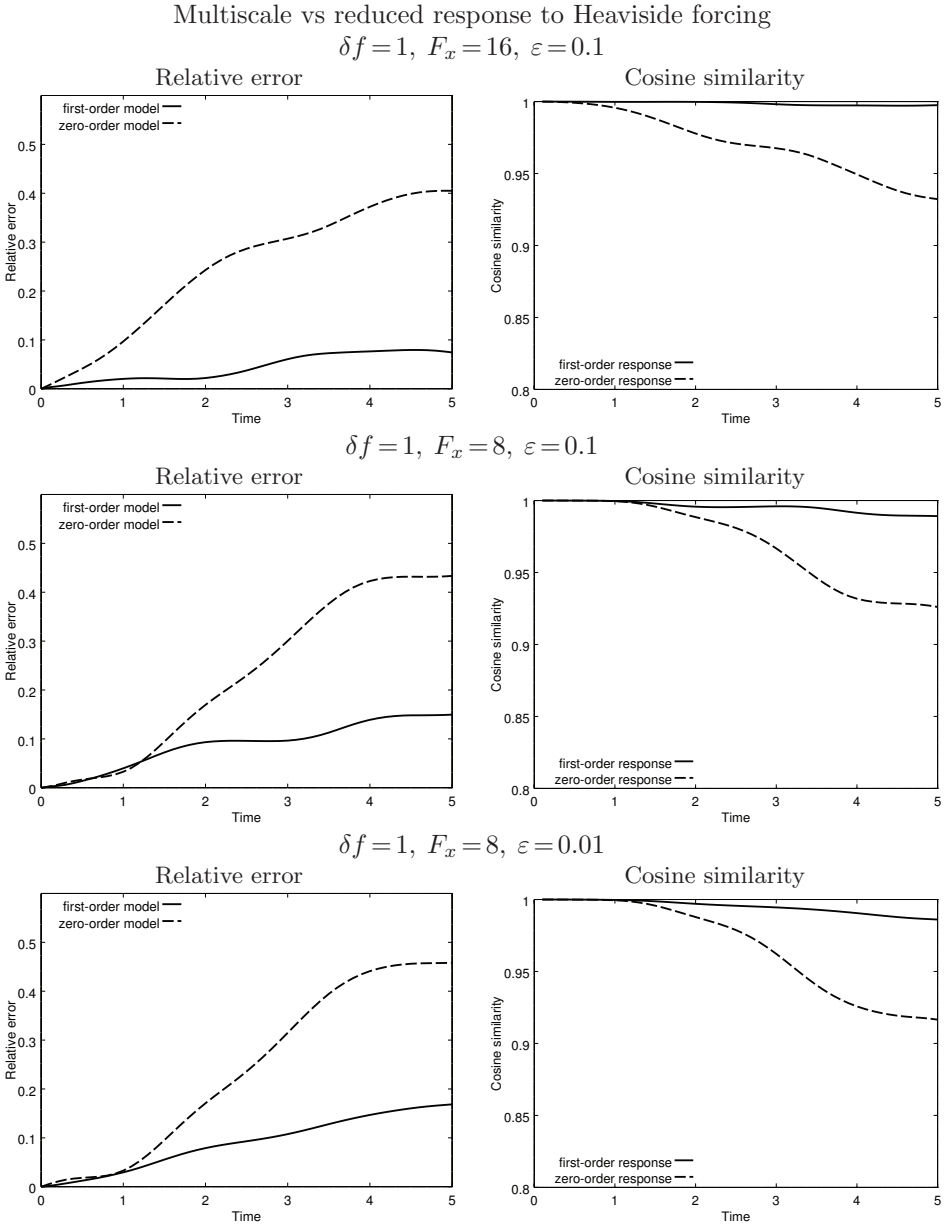

FIG. 6.9. *Comparison of multiscale and reduced system mean responses* $\delta\langle \boldsymbol{x}\rangle(t)$ *to Heaviside forcing. Relative error* (6.5) *on the left, cosine similarity* (6.6) *on the right.*

time

$$E(t) = \frac{\|\delta\langle \boldsymbol{x}\rangle(t) - \delta\langle \boldsymbol{x}\rangle_A(t)\|}{\|\delta\langle \boldsymbol{x}\rangle(t)\|} \tag{6.5}$$

and the cosine similarity

$$E(t) = \frac{\delta\langle \boldsymbol{x}\rangle(t) \cdot \delta\langle \boldsymbol{x}\rangle_A(t)}{\|\delta\langle \boldsymbol{x}\rangle(t)\| \|\delta\langle \boldsymbol{x}\rangle_A(t)\|} \tag{6.6}$$

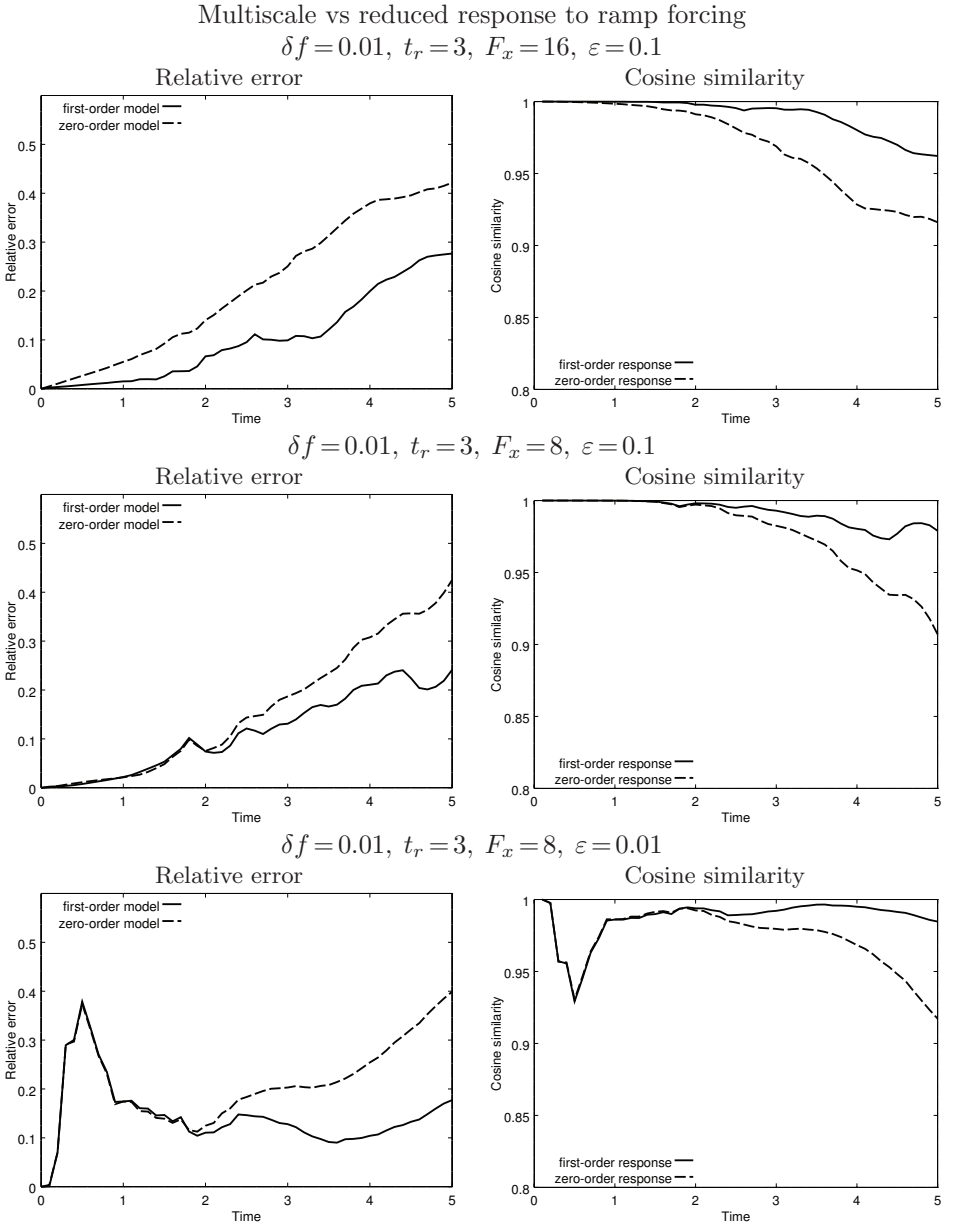

FIG. 6.10. *Comparison of multiscale and reduced system mean responses* $\delta\langle \boldsymbol{x} \rangle(t)$ *to ramp forcing with* $t_r = 3$. *Relative error* (6.5) *on the left, cosine similarity* (6.6) *on the right.*

of the mean responses $\delta\langle \boldsymbol{x} \rangle(t)$ and $\delta\langle \boldsymbol{x} \rangle_A(t)$ of the multiscale and reduced systems, respectively. These plots are shown in figures 6.8–6.11 for first-order and zero-order reduced systems.

We observe that the first-order reduced system response is a much closer approximation to the multiscale response than the corresponding zero-order response in all cases. In these regimes, the relative error of the first-order response is limited to about 30% for small forcings and about 20% for the ramp forcing, while, in the zero-order

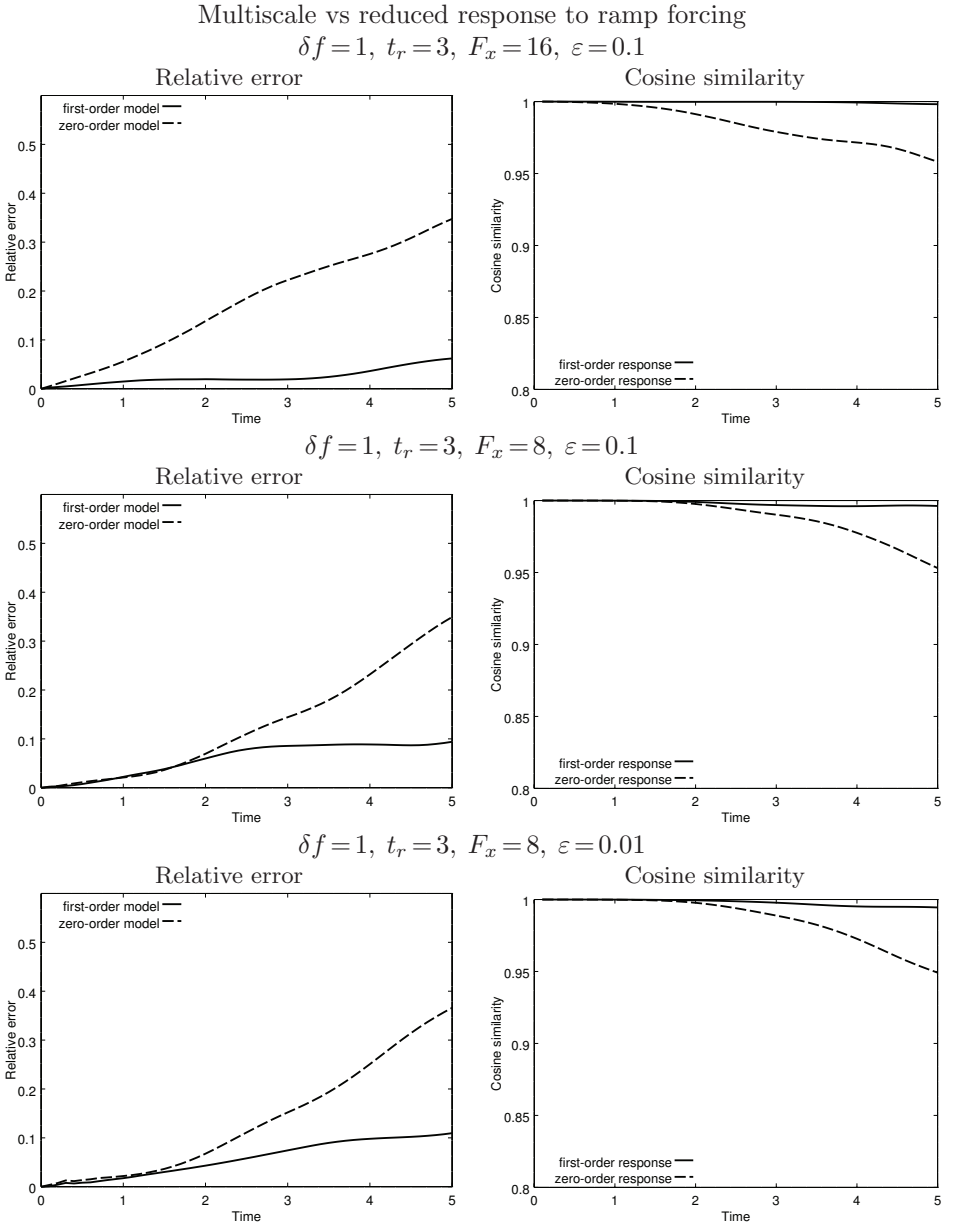

FIG. 6.11. *Comparison of multiscale and reduced system mean responses* $\delta\langle \boldsymbol{x}\rangle(t)$ *to ramp forcing with* $t_r = 3$. *Relative error* (6.5) *on the left, cosine similarity* (6.6) *on the right.*

system, the difference can exceed 50% at $t = 5$ time units.

Note the plots for small ramp forcing in Figure 6.10, where we see a spike in the response differences shortly after the onset of forcing in the weakly chaotic regime ($F_x = 8, F_y = 12$) with large timescale separation ($\varepsilon = 0.01$) in the multiscale system. In this regime, the small nonlinear fluctuations of the multiscale system develop rapidly and are relatively large compared to the ramp forcing for t near zero, so the relative error of the reduced system responses is large. As the ramp forcing increases, the large features

of the response become manifest and the above contribution becomes negligible.

7. Summary

In this work, we studied the statistical properties and response to small external perturbations of multiscale dynamics and their reduced models for slow variables only. We elucidated a set of criteria for statistical properties of the multiscale and reduced systems which facilitated similarity of responses of both systems to small external perturbations. It was shown that the similarity of marginal distribution densities of slow variables and their time autocorrelation functions controlled the similarity of responses to small external perturbations of both systems.

As in [4], here we demonstrated that including a first-order correction term to a standard closure approximation for a nonlinear chaotic two-time system offered distinct improvements over the zero-order closure in capturing large-scale features of the slow dynamics. In particular, this reduced system was able to accurately capture the distribution density of solutions as well as the mean state response of the system to simple forcing perturbations. This correction term was relatively easy to generate, requiring only simple statistical calculations of the uncoupled fast system for an appropriate set of fixed parameters, and the resulting reduced system required much less computational resources than the underlying multiscale system.

Here, the linear response closure derivation and numerical results have been presented only for the special case of linear coupling between slow and fast systems, but this derivation has been extended to systems with nonlinear and multiplicative coupling [6], encompassing a much broader set of potential applications. In future work we hope to extend similar results to these more general systems and to test the robustness of this method in applications to a large variety of multiscale problems.

Appendix A. Linear response formula. Here, we derive the linear response formula (3.5). Consider the dynamical system given by the ODE system

$$\frac{\mathrm{d}\boldsymbol{x}}{\mathrm{d}t} = \boldsymbol{F}(\boldsymbol{x}), \qquad \boldsymbol{x}(t) = \phi^t \boldsymbol{x}, \tag{A.1}$$

where $\boldsymbol{F}: \mathbb{R}^N \to \mathbb{R}^N$ is a differential vector field and ϕ^t the flow operator generated by $\boldsymbol{F}$. Let μ be an ergodic invariant probability measure for this system so that, for any smooth function $h(\boldsymbol{x})$ and any t,

$$\langle h \rangle = \langle h \circ \phi^t \rangle, \tag{A.2}$$

where

$$\langle h \rangle = \int h(\boldsymbol{x}) \mathrm{d}\mu(\boldsymbol{x}). \tag{A.3}$$

Now, suppose system (A.1) is perturbed by a small forcing term of the form

$$\frac{\mathrm{d}\boldsymbol{x}}{\mathrm{d}t} = \boldsymbol{F}(\boldsymbol{x}) + w(\boldsymbol{x}) \delta \boldsymbol{f}(t), \qquad \boldsymbol{x}(t) = \hat{\phi}^t \boldsymbol{x}, \tag{A.4}$$

where w is an $N \times K$ matrix and $\delta \boldsymbol{f}$ is a K-dimensional vector such that $\delta \boldsymbol{f}(t) = 0$ for $t < 0$, and where $\hat{\phi}^t$ is the flow operator corresponding to this system with initial condition at $t = 0$. We are interested in the response of $\langle h \rangle$ following the onset of this perturbation:

$$\delta \langle h \rangle(t) = \int \Big(h(\hat{\phi}^t \boldsymbol{x}) - h(\phi^t \boldsymbol{x}) \Big) \mathrm{d}\mu(\boldsymbol{x}). \tag{A.5}$$

This response will depend in some way on the forcing, $\delta\langle h\rangle(t) = \mathcal{V}(w, \delta f)$, which is *a priori* unknown. However, when the forcing is small enough, we expect this dependence to be approximately linear. Expanding with respect to $\delta\phi^t\boldsymbol{x} = \hat{\phi}^t\boldsymbol{x} - \phi^t\boldsymbol{x}$ and discarding higher-order terms, we have

$$\delta\langle h\rangle(t) \approx \int \nabla h(\phi^t\boldsymbol{x})\delta\phi^t\boldsymbol{x}\mathrm{d}\mu(\boldsymbol{x}). \tag{A.6}$$

Furthermore, we make a linear approximation to $\delta\phi^t\boldsymbol{x}$. Subtracting (A.1) from (A.4) and linearizing this difference, we have

$$\frac{\partial}{\partial t}\delta\phi^t\boldsymbol{x} \approx J(\phi^t\boldsymbol{x})\delta\phi^t\boldsymbol{x} + w(\phi^t\boldsymbol{x})\delta\boldsymbol{f}(t), \qquad \delta\phi^0\boldsymbol{x} = 0, \tag{A.7}$$

where $J = \frac{\partial \boldsymbol{F}}{\partial \boldsymbol{x}}$ is the Jacobian of $\boldsymbol{F}$. The solution to this linear ODE is given by Duhamel's principle:

$$\delta\phi^t\boldsymbol{x} = \int_0^t \exp\left(\int_\tau^t J(\phi^s\boldsymbol{x})\mathrm{d}s\right) w(\phi^\tau\boldsymbol{x})\delta\boldsymbol{f}(\tau)\mathrm{d}\tau. \tag{A.8}$$

Defining the tangent map as $T^t_{\boldsymbol{x}} = \frac{\partial\phi^t\boldsymbol{x}}{\partial\boldsymbol{x}}$ and differentiating (A.1) with respect to $\boldsymbol{x}$, we have

$$\frac{\partial}{\partial t}T^t_{\boldsymbol{x}} = J(\phi^t\boldsymbol{x})T^t_{\boldsymbol{x}}, \qquad T^0_{\boldsymbol{x}} = \mathrm{Id}_N. \tag{A.9}$$

Since $\phi^t = \phi^{t-\tau}\circ\phi^\tau$ for all τ, by the chain rule of differentiation, we have $T^t_{\boldsymbol{x}} = T^{t-\tau}_{\phi^\tau\boldsymbol{x}}T^\tau_{\boldsymbol{x}}$. Substituting this into (A.9) and multiplying both sides by $T^{-\tau}_{\phi^\tau\boldsymbol{x}}$, we have

$$\frac{\partial}{\partial t}T^{t-\tau}_{\phi^\tau\boldsymbol{x}} = J(\phi^t\boldsymbol{x})T^{t-\tau}_{\phi^\tau\boldsymbol{x}}, \tag{A.10}$$

whose solution is given by

$$T^{t-\tau}_{\phi^\tau\boldsymbol{x}} = \exp\left(\int_\tau^t J(\phi^s\boldsymbol{x})\mathrm{d}s\right). \tag{A.11}$$

From (A.8), we have

$$\delta\phi^t\boldsymbol{x} = \int_0^t T^{t-\tau}_{\phi^\tau\boldsymbol{x}} w(\phi^\tau\boldsymbol{x})\delta\boldsymbol{f}(\tau)\mathrm{d}\tau. \tag{A.12}$$

Substituting this is into (A.6), we obtain

$$\begin{aligned}\delta\langle h\rangle(t) &= \int_0^t \left[\int \nabla h(\phi^t\boldsymbol{x})T^{t-\tau}_{\phi^\tau\boldsymbol{x}} w(\phi^\tau\boldsymbol{x})\mathrm{d}\mu(\boldsymbol{x})\right]\delta\boldsymbol{f}(\tau)\mathrm{d}\tau \\ &= \int_0^t \left[\int \nabla h(\phi^{t-\tau}\boldsymbol{x})T^{t-\tau}_{\phi^{t-\tau}\boldsymbol{x}} w(\boldsymbol{x})\mathrm{d}\mu(\boldsymbol{x})\right]\delta\boldsymbol{f}(\tau)\mathrm{d}\tau,\end{aligned} \tag{A.13}$$

where the second equality comes from the fact that μ is an invariant measure for the system. Hence, we have the linear response relation

$$\begin{aligned}\delta\langle h\rangle(t) &= \int_0^t R(t-\tau)\delta\boldsymbol{f}(\tau)\mathrm{d}\tau, \\ R(t) &= \int \nabla h(\phi^t\boldsymbol{x})T^t_{\boldsymbol{x}} w(\boldsymbol{x})\mathrm{d}\mu(\boldsymbol{x}) \\ &= \int \frac{\partial}{\partial\boldsymbol{x}}\left(h(\phi^t\boldsymbol{x})\right) w(\boldsymbol{x})\mathrm{d}\mu(\boldsymbol{x}).\end{aligned} \tag{A.14}$$

For more details, see [1–3, 8–11, 44].

Appendix B. Reduced model formula for slow variables of two-timescale systems with linear coupling. Consider a two-timescale dynamical system given by the following system of ODEs with linear coupling between the slow variables $\boldsymbol{x} \in \mathbb{R}^{N_x}$ and fast variables $\boldsymbol{y} \in \mathbb{R}^{N_y}$:

$$\begin{cases} \dfrac{\mathrm{d}\boldsymbol{x}}{\mathrm{d}t} = \boldsymbol{f}(\boldsymbol{x}) + \boldsymbol{L}_y \boldsymbol{y}, \\ \dfrac{\mathrm{d}\boldsymbol{y}}{\mathrm{d}t} = \boldsymbol{g}(\boldsymbol{y}) + \boldsymbol{L}_x \boldsymbol{x}, \end{cases} \tag{B.1}$$

where $\boldsymbol{f}$ and $\boldsymbol{g}$ are differentiable functions and $\boldsymbol{L}_x$ and $\boldsymbol{L}_y$ are constant matrices. If the $\boldsymbol{y}$-variables are sufficiently fast compared to the $\boldsymbol{x}$-variables, one can use the averaging formalism [38, 39, 46, 47] to write an averaged system for slow variables alone:

$$\frac{\mathrm{d}\boldsymbol{x}}{\mathrm{d}t} = \boldsymbol{f}(\boldsymbol{x}) + \boldsymbol{L}_y \bar{\boldsymbol{z}}(\boldsymbol{x}), \tag{B.2}$$

where $\bar{\boldsymbol{z}}(\boldsymbol{x})$ is the statistical mean state of fast limiting system

$$\frac{\mathrm{d}\boldsymbol{z}}{\mathrm{d}t} = \boldsymbol{g}(\boldsymbol{z}) + \boldsymbol{L}_x \boldsymbol{x}, \qquad \boldsymbol{z}(t) = \varphi^t(\boldsymbol{z}), \tag{B.3}$$

with $\boldsymbol{x}$ as a constant parameter. In general, the dependence of the mean state $\bar{\boldsymbol{z}}(\boldsymbol{x})$ on $\boldsymbol{x}$ is not explicitly known. We will approximate it with a linear expansion, as in [4, 7]:

$$\bar{\boldsymbol{z}}(\boldsymbol{x}) \approx \bar{\boldsymbol{z}}^* + \boldsymbol{\mathcal{C}} \boldsymbol{L}_x (\boldsymbol{x} - \boldsymbol{x}^*), \tag{B.4}$$

where $\boldsymbol{x}^*$ is the statistical mean state of the slow variables in the multiscale system in (B.1) or another appropriate reference state and where $\bar{\boldsymbol{z}}^* = \bar{\boldsymbol{z}}(\boldsymbol{x}^*)$, with the constant matrix $\boldsymbol{\mathcal{C}}$ to be computed as follows.

If we perturb the fast limiting system (B.3) at $\boldsymbol{x} = \boldsymbol{x}^*$ by adding the quantity $\boldsymbol{L}_x(\boldsymbol{x} - \boldsymbol{x}*)$ to the right-hand side, the linear response of $\bar{\boldsymbol{z}}^*$ is given by (A.14):

$$\begin{aligned} \delta \bar{\boldsymbol{z}}^*(t) &= \int_0^t R(\tau) \mathrm{d}\tau \ \boldsymbol{L}_x (\boldsymbol{x} - \boldsymbol{x}^*), \\ R(t) &= \int \frac{\partial}{\partial \boldsymbol{z}} \left(\varphi^t \boldsymbol{z} \right) \mathrm{d}\mu_{\boldsymbol{x}^*}(\boldsymbol{z}), \end{aligned} \tag{B.5}$$

where $\mu_{\boldsymbol{x}^*}$ is an invariant measure of system (B.3) with $\boldsymbol{x} = \boldsymbol{x}^*$. If $\mu_{\boldsymbol{x}^*}$ is absolutely continuous with respect to the Lebesgue measure with distribution density $\rho(\boldsymbol{z}; \boldsymbol{x}^*)$, we can write the response kernel as

$$\boldsymbol{R}(t) = \int \frac{\partial}{\partial \boldsymbol{z}} \left(\varphi^t \boldsymbol{z} \right) \rho(\boldsymbol{z}; \boldsymbol{x}^*) \mathrm{d}\boldsymbol{z}. \tag{B.6}$$

While deterministic processes may not have Lebesgue-continuity of their invariant measures [42, 43, 50], a small amount of random noise, which is always present in real-world complex geophysical dynamics and numerical roundoff error, usually ensures the existence of the distribution density. Integration by parts yields

$$\boldsymbol{R}(t) = -\int \varphi^t \boldsymbol{z} \frac{\partial \rho(\boldsymbol{z}; \boldsymbol{x}^*)}{\partial \boldsymbol{z}} \mathrm{d}\boldsymbol{z}. \tag{B.7}$$

Denoting by Σ the covariance matrix of the fast limiting system (B.3) with $\boldsymbol{x}=\boldsymbol{x}^*$, we take a simplifying approximation of $\rho(\boldsymbol{z};\boldsymbol{x}^*)$ to be a Gaussian distribution:

$$\rho(\boldsymbol{z};\boldsymbol{x}^*)=-\left(\sqrt{2\pi\det\Sigma}\right)^{-N_y}\exp\left(-\frac{1}{2}(\boldsymbol{z}-\overline{\boldsymbol{z}}^*)\Sigma^{-1}(\boldsymbol{z}-\overline{\boldsymbol{z}}^*)\right). \tag{B.8}$$

Then, we have

$$\begin{aligned}\boldsymbol{R}(t)&=\int\varphi^t\boldsymbol{z}(\boldsymbol{z}-\bar{\boldsymbol{z}}^*)^T\rho(\boldsymbol{z};\boldsymbol{x}^*)\mathrm{d}\boldsymbol{z}\ \Sigma^{-1}\\&=\int\varphi^t\boldsymbol{z}(\boldsymbol{z}-\bar{\boldsymbol{z}}^*)^T\mathrm{d}\mu_{\boldsymbol{x}^*}(z)\ \Sigma^{-1}.\end{aligned} \tag{B.9}$$

This results in the quasi-Gaussian linear response operator, which is a good approximation when the dynamics in (B.3) are strongly chaotic and rapidly mixing [1–3, 8–11, 28, 40]. Given time series data $\boldsymbol{z}(t)$ for the fast limiting system (B.3), this is simply calculated as

$$\boldsymbol{R}(t)=\int_0^\infty\boldsymbol{z}(\tau+t)(\boldsymbol{z}(\tau)-\bar{\boldsymbol{z}}^*)^T\mathrm{d}\tau\ \Sigma^{-1}, \tag{B.10}$$

with sample mean and covariance

$$\begin{aligned}\bar{\boldsymbol{z}}^*&=\int_0^\infty\boldsymbol{z}(\tau)\mathrm{d}\tau,\\\Sigma&=\int_0^\infty\boldsymbol{z}(\tau)(\boldsymbol{z}(\tau)-\bar{\boldsymbol{z}}^*)^T\mathrm{d}\tau,\end{aligned} \tag{B.11}$$

respectively.

Acknowledgment. Rafail Abramov was supported by the National Science Foundation CAREER grant DMS-0845760, and the Office of Naval Research grants N00014-09-0083 and 25-74200-F6607. Marc Kjerland was supported as a Research Assistant through the National Science Foundation CAREER grant DMS-0845760.

REFERENCES

[1] R.V. Abramov, *Short-time linear response with reduced-rank tangent map*, Chin. Ann. Math., 30B(5), 447–462, 2009.
[2] R.V. Abramov, *Approximate linear response for slow variables of deterministic or stochastic dynamics with time scale separation*, J. Comput. Phys., 229(20), 7739–7746, 2010.
[3] R.V. Abramov, *Improved linear response for stochastically driven systems*, Front. Math. China, 7(2), 199–216, 2012.
[4] R.V. Abramov, *A simple linear response closure approximation for slow dynamics of a multiscale system with linear coupling*, Multiscale Model. Simul., 10(1), 28–47, 2012.
[5] R.V. Abramov, *Suppression of chaos at slow variables by rapidly mixing fast dynamics through linear energy-preserving coupling*, Commun. Math. Sci., 10(2), 595–624, 2012.
[6] R.V. Abramov, *A simple closure approximation for slow dynamics of a multiscale system: Nonlinear and multiplicative coupling*, Multiscale Model. Simul., 11(1), 134–151, 2013.
[7] R.V. Abramov, *A simple stochastic parameterization for reduced models of multiscale dynamics*, Fluids, submitted, 2015.
[8] R.V. Abramov and A.J. Majda, *Blended response algorithms for linear fluctuation-dissipation for complex nonlinear dynamical systems*, Nonlinearity, 20, 2793–2821, 2007.
[9] R.V. Abramov and A.J. Majda, *New approximations and tests of linear fluctuation-response for chaotic nonlinear forced-dissipative dynamical systems*, J. Nonlin. Sci., 18(3), 303–341, 2008.

[10] R.V. Abramov and A.J. Majda, *New algorithms for low frequency climate response*, J. Atmos. Sci., 66, 286–309, 2009.
[11] R.V. Abramov and A.J. Majda, *Low frequency climate response of quasigeostrophic wind-driven ocean circulation*, J. Phys. Oceanogr., 42, 243–260, 2012.
[12] R. Azencott, A. Beri, and I. Timofeyev, *Sub-sampling and parametric estimation for multiscale dynamics*, Commun. Math. Sci., 11(4), 939–970, 2013.
[13] G. Branstator, *Low-frequency patterns induced by stationary waves*, J. Atmos. Sci., 47, 629–648, 1990.
[14] G. Branstator and J. Berner, *Linear and nonlinear signatures in planetary wave dynamics of an AGCM: phase space tendencies*, J. Atmos. Sci., 62, 1792–1811, 2005.
[15] R. Buizza, M. Miller, and T. Palmer, *Stochastic representation of model uncertainty in the ECMWF Ensemble Prediction System*, Q. J. R. Meteor. Soc., 125, 2887–2908, 1999.
[16] D.T. Crommelin and E. Vanden-Eijnden, *Subgrid scale parameterization with conditional Markov chains*, J. Atmos. Sci., 65, 2661–2675, 2008.
[17] I. Fatkullin and E. Vanden-Eijnden, *A computational strategy for multiscale systems with applications to Lorenz 96 model*, J. Comp. Phys., 200, 605–638, 2004.
[18] C. Franzke and A.J. Majda, *Low-order stochastic mode reduction for a prototype atmospheric GCM*, J. Atmos. Sci., 63, 457–479, 2006.
[19] C. Franzke, A.J. Majda, and E. Vanden-Eijnden, *Low-order stochastic model reduction for a realistic barotropic model climate*, J. Atmos. Sci., 62, 1722–1745, 2005.
[20] A. Gritsun and G. Branstator, *Climate response using a three-dimensional operator based on the fluctuation-dissipation theorem*, J. Atmos. Sci., 64, 2558–2575, 2006.
[21] A. Gritsun and V. Dymnikov, *Barotropic atmosphere response to small external actions. theory and numerical experiments*, Atmos. Ocean Phys., 35(5), 511–525, 1999.
[22] K. Hasselmann, *Stochastic climate models, part I, theory*, Tellus, 28, 473–485, 1976.
[23] M.A. Katsoulakis and G.D. Vlachos, *Hierarchical kinetic Monte Carlo simulations for diffusion of interacting molecules*, J. Chem. Phys., 112, 9412–9427, 2003.
[24] B. Khouider, A.J. Majda, and M.A. Katsoulakis, *Coarse grained stochastic models for tropical convection*, Proc. Natl. Acad. Sci., 100, 11941–11946, 2003.
[25] S. Kravtsov, D. Kondrashov, and M. Ghil, *Multilevel regression modeling of nonlinear processes: Derivation and applications to climatic variability*, J. Clim., 18(21), 4404–4424, 2005.
[26] S. Kullback and R. Leibler, *On information and sufficiency*, Ann. Math. Stat., 22, 79–86, 1951.
[27] E. Lorenz, *Predictability: A Problem Partly Solved*, in Proceedings of the Seminar on Predictability, Shinfield Park, Reading, England, 1996. ECMWF.
[28] A.J. Majda, R.V Abramov, and M.J. Grote, *Information Theory and Stochastics for Multiscale Nonlinear Systems*, CRM Monograph Series of Centre de Recherches Mathématiques, Université de Montréal, American Mathematical Society, 25, 2005. ISBN 0-8218-3843-1.
[29] A.J. Majda, C. Franzke, and D.T. Crommelin, *Normal forms for reduced stochastic climate models*, Proc. Natl. Acad. Sci., 97, 12413–12417, 2009.
[30] A.J. Majda, B. Gershgorin, and Y. Yuan, *Low frequency response and fluctuation-dissipation theorems: Theory and practice*, J. Atmos. Sci., 67, 1186–1201, 2010.
[31] A.J. Majda and B. Khouider, *Stochastic and mesoscopic models for tropical convection*, Proc. Natl. Acad. Sci., 99, 1123–1128, 2002.
[32] A.J. Majda, I. Timofeyev, and E. Vanden-Eijnden, *Models for stochastic climate prediction*, Proc. Natl. Acad. Sci., 96, 14687–14691, 1999.
[33] A.J. Majda, I. Timofeyev, and E. Vanden-Eijnden, *A mathematical framework for stochastic climate models*, Commun. Pure Appl. Math., 54, 891–974, 2001.
[34] A.J. Majda, I. Timofeyev, and E. Vanden-Eijnden, *A priori tests of a stochastic mode reduction strategy*, Physica D, 170, 206–252, 2002.
[35] A.J. Majda, I. Timofeyev, and E. Vanden-Eijnden, *Systematic strategies for stochastic mode reduction in climate*, J. Atmos. Sci., 60, 1705–1722, 2003.
[36] M. Newman, P.D. Sardeshmukh, and C. Penland, *Stochastic forcing of the wintertime extratropical flow*, J. Atmos. Sci., 54, 435–455, 1997.
[37] T. Palmer, *A nonlinear dynamical perspective on model error: A proposal for nonlocal stochastic-dynamic parameterization in weather and climate prediction models*, Q. J. R. Meteor. Soc., 127, 279–304, 2001.
[38] G. Papanicolaou, *Introduction to the asymptotic analysis of stochastic equations*, R. DiPrima (ed.), Modern modeling of continuum phenomena, Lectures in Applied Mathematics, Amer. Math. Soc., 16, 1977.
[39] G. Pavliotis and A. Stuart, *Multiscale Methods: Averaging and Homogenization*, Springer, 2008.
[40] H. Risken, *The Fokker-Planck Equation*, Springer-Verlag, New York, Secnd Edition, 1989.
[41] Y. Rubner, C. Tomasi, and L.J. Guibas, *The earth mover's distance as a metric for image*

retrieval, Int. J. Comput. Vision, 40(2), 99–121, 2000.
[42] D. Ruelle, *Chaotic Evolution and Strange Attractors*, Cambridge University Press, 1989.
[43] D. Ruelle, *Differentiation of SRB states*, Commun. Math. Phys., 187, 227–241, 1997.
[44] D. Ruelle, *General linear response formula in statistical mechanics, and the fluctuation-dissipation theorem far from equilibrium*, Phys. Lett. A, 245, 220–224, 1998.
[45] G. Uhlenbeck and L. Ornstein, *On the theory of the Brownian motion*, Phys. Rev., 36, 823–841, 1930.
[46] E. Vanden-Eijnden, *Numerical techniques for multiscale dynamical systems with stochastic effects*, Commun. Math. Sci., 1, 385–391, 2003.
[47] V.M. Volosov, *Averaging in systems of ordinary differential equations*, Russian Math. Surveys, 17, 1–126, 1962.
[48] J.S. Whitaker and P.D. Sardeshmukh, *A linear theory of extratropical synoptic eddy statistics*, J. Atmos. Sci., 55, 237–258, 1998.
[49] D. Wilks, *Effects of stochastic parameterizations in the Lorenz' 96 system*, Q. J. R. Meteorol. Soc., 131, 389–407, 2005.
[50] L.-S. Young, *What are SRB measures, and which dynamical systems have them?* J. Stat. Phys., 108(5-6), 733–754, 2002.
[51] Y. Zhang and I.M. Held, *A linear stochastic model of a GCM's midlatitude storm tracks*, J. Atmos. Sci., 56, 3416–3435, 1999.